



Calhoun: The NPS Institutional Archive

Theses and Dissertations

Thesis Collection

1993-09

Mesoscale frontal evolution of the ERICA IOP-5A cyclone

Cameron, Steven R.

Monterey, California. Naval Postgraduate School

<http://hdl.handle.net/10945/27129>



Calhoun is a project of the Dudley Knox Library at NPS, furthering the precepts and goals of open government and government transparency. All information contained herein has been approved for release by the NPS Public Affairs Officer.

Dudley Knox Library / Naval Postgraduate School
411 Dyer Road / 1 University Circle
Monterey, California USA 93943

<http://www.nps.edu/library>

NOX LIBRARY

STATE SCHOOL

DATE

33943-5101

Approved for public release; distribution is unlimited.

Mesoscale Frontal Evolution of
the ERICA IOP-5A Cyclone

by

Steven R. Cameron
Lieutenant Commander, United States Navy
B.S., West Virginia University

Submitted in partial fulfillment
of the requirements for the degree of

MASTER OF SCIENCE IN METEOROLOGY AND PHYSICAL OCEANOGRAPHY

from the

NAVAL POSTGRADUATE SCHOOL
September 1993

| REPORT DOCUMENTATION PAGE | | | | |
|---|-------|--|---|---|
| 1a Report Security Classification: Unclassified | | 1b Restrictive Markings | | |
| 2a Security Classification Authority | | 3 Distribution/Availability of Report | | |
| 2b Declassification/Downgrading Schedule | | Approved for public release; distribution is unlimited. | | |
| 4 Performing Organization Report Number(s) | | 5 Monitoring Organization Report Number(s) | | |
| 6a Name of Performing Organization Naval Postgraduate School | | 6b Office Symbol (if applicable) 35 | | 7a Name of Monitoring Organization Naval Postgraduate School |
| 6c Address (city, state, and ZIP code) Monterey CA 93943-5002 | | 7b Address (city, state, and ZIP code) Monterey CA 93943-5002 | | |
| 8a Name of Funding/Sponsoring Organization | | 6b Office Symbol (if applicable) | | 9 Procurement Instrument Identification Number |
| Address (city, state, and ZIP code) | | 10 Source of Funding Numbers | | |
| | | Program Element No | Project No | Task No |
| | | Work Unit Accession N | | |
| 11 Title (include security classification) MESOSCALE FRONTAL EVOLUTION OF THE ERICA IOP-5A CYCLONE | | | | |
| 12 Personal Author(s) Steven R. Cameron | | | | |
| 13a Type of Report Master's Thesis | | 13b Time Covered From To | 14 Date of Report (year, month, day) 1993, September | 15 Page Count 81 |
| 16 Supplementary Notation The views expressed in this thesis are those of the author and do not reflect the official policy or position of the Department of Defense or the U.S. Government. | | | | |
| 17 Cosati Codes | | 18 Subject Terms (continue on reverse if necessary and identify by block number) | | |
| Field | Group | Subgroup | Experiment on Rapidly Intensifying Cyclones over the Atlantic (ERICA) IOP-5A, rapid cyclogenesis, mesoscale frontal evolution | |
| | | | | |
| 19 Abstract (continue on reverse if necessary and identify by block number) | | | | |
| <p>A synoptic investigation was conducted of the rapid coastal cyclogenesis that occurred during Intensive Observation Period (IOP) 5A of the Experiment on Rapidly Intensifying Cyclones over the Atlantic (ERICA). Navy Operational Regional Analysis and Prediction System (NORAPS) forecasts were examined in order to study the mesoscale frontal evolution associated with this rapidly deepening coastal cyclone. The ability of the NORAPS forecasts to accurately depict the frontal positions and intensity was also investigated.</p> <p>The frontal evolution showed characteristics of a classical occlusion, similar to the Norwegian cyclone model and of marine frontal structure as discussed by Shapiro and Keyser (1990). The frontal evolution was highly influenced by the prior existence of strong arctic and coastal fronts. These fronts intensified during the course of the storm development and did not develop as a result of the cyclogenesis.</p> <p>The NORAPS model forecasts were compared against satellite imagery, station reports and observed soundings taken during the ERICA study. The NORAPS model was found to be an excellent tool for forecasting the mesoscale frontal structure and intensity of this rapidly deepening coastal cyclone.</p> | | | | |
| 20 Distribution/Availability of Abstract XX unclassified/unlimited same as report DTIC users | | 21 Abstract Security Classification Unclassified | | |
| 22a Name of Responsible Individual Carlyle H. Wash | | 22b Telephone (include Area Code) (408) 656-2269 | | 22c Office Symbol MR/Wx |

ABSTRACT

A synoptic investigation was conducted of the rapid coastal cyclogenesis that occurred during Intensive Observation Period (IOP) 5A of the Experiment on Rapidly Intensifying Cyclones over the Atlantic (ERICA). Navy Operational Regional Analysis and Prediction System (NORAPS) forecasts were examined in order to study the mesoscale frontal evolution associated with this rapidly deepening coastal cyclone. The ability of the NORAPS forecasts to accurately depict the frontal positions and intensity was also investigated.

The frontal evolution showed characteristics of a classical occlusion, similar to the Norwegian cyclone model and of marine frontal structure as discussed by Shapiro and Keyser (1990). The frontal evolution was highly influenced by the prior existence of strong arctic and coastal fronts. These fronts intensified during the course of the storm development and did not develop as a result of the cyclogenesis.

The NORAPS model forecasts were compared against satellite imagery, station reports and observed soundings taken during the ERICA study. The NORAPS model was found to be an excellent tool for forecasting the mesoscale frontal structure and intensity of this rapidly deepening coastal cyclone.

1/18/83
C1977
C.1

TABLE OF CONTENTS

| | | |
|------|---|----|
| I. | INTRODUCTION | 1 |
| II. | BACKGROUND | 4 |
| A. | REVIEW OF CYCLOGENESIS | 4 |
| B. | ASPECTS OF THE EXPERIMENT ON RAPIDLY INTENSIFYING CYCLONES OVER THE ATLANTIC (ERICA) | 6 |
| C. | MESOSCALE FRONTAL STRUCTURE OF CYCLONES | 7 |
| D. | THE NAVY OPERATIONAL REGIONAL ATMOSPHERIC PREDICTION SYSTEM (NORAPS) | 9 |
| III. | FRONTAL EVOLUTION OF ERICA IOP-5A | 11 |
| A. | 20/1200Z January 1989 | 15 |
| B. | 20/1800Z January 1989 | 16 |
| C. | 21/0000Z January 1989 | 18 |
| D. | 21/0300Z January 1989 | 20 |
| E. | 21/0600Z January 1989 | 20 |
| F. | 21/1200Z January 1989 | 22 |
| G. | 21/1800Z January 1989 | 26 |
| H. | 21/2100Z January 1989 | 28 |
| I. | 22/0000Z January 1989 | 28 |
| J. | Early Mesoscale Development | 29 |
| K. | Summary | 31 |

| | |
|---|----|
| IV. CONCLUSIONS AND RECOMMENDATIONS | 34 |
| A. CONCLUSIONS | 34 |
| B. RECOMMENDATIONS | 35 |
| APPENDIX | 37 |
| LIST OF REFERENCES | 71 |
| INITIAL DISTRIBUTION LIST | 73 |

ACKNOWLEDGEMENTS

I would like to express my sincere thanks to Professor Carlyle Wash for sharing his time, experience and guidance in support of my thesis research. I would also like to thank Professor Paul Hirschberg for his technical support and assistance in this study. Additionally, thanks are due to Mr. Rolf Langland (and the Naval Research Laboratory Monterey in general) for preparing the ERICA IOP-5A NORAPS analyses and NORAPS forecasts studied in this thesis.

Finally, I would like to thank Ms. Mary Jordan for her efforts in cataloging the ERICA data sets and for the assistance she provided to me while working with those data sets.

I. INTRODUCTION

Rapid oceanic cyclogenesis adversely impacts military operations by disrupting the use and defense of the sea lines of communication. These storms are associated with high winds and waves that also restrict visibility and pose substantial danger to both personnel and property. Unfortunately, since the oceans are regions where observational data coverage is poor, accurate predictions of rapidly deepening cyclones are often not obtained. In addition, although the large-scale processes that contribute to rapid cyclogenesis are well documented (Uccellini, 1990), the role that mesoscale processes play in the development and evolution of explosively developing cyclones remains a research issue. Moreover, mesoscale features (e.g. fronts) can have a significant impact on local weather, but may not be represented well by operational numerical models.

The damage caused by the weather associated with a rapidly developing surface cyclone can be extensive. Therefore, it is imperative that forecasts of the occurrence and location of rapid cyclogenesis, and the attendant mesoscale circulation features be as accurate and timely as possible. For example, an accurate depiction of the mesoscale structure of a developing cyclone would allow for the issuance of more precise and detailed forecast warnings. This need for a

clearer understanding of the synoptic and mesoscale dynamics of rapid cyclogenesis led to the Office of Naval Research (ONR) sponsored Experiment on Rapidly Intensifying Cyclones over the Atlantic (ERICA) during the winter of 1988-1989. The extensive data set obtained from this experiment provides an excellent opportunity to investigate the factors that contribute to rapid cyclogenesis. During the 1988-1989 observation period (December 1988 until February 1989) of ERICA, nine cyclone cases were studied.

The goal of this thesis is to explore aspects of one particularly interesting cyclone case observed during ERICA intensive observation period (IOP) 5A. This storm (IOP 5A) developed along the New England coast and had a deepening rate of 15 mb in six hours (Spinelli 1992). Specifically, an assessment of the Navy Operational Regional Atmospheric Prediction System (NORAPS) will be conducted to evaluate the capability of the model to predict mesoscale features associated with the cyclone development. In addition, a comparison between the frontal evolutions associated with rapidly deepening ocean storms and the coastal IOP 5A storm will be performed to determine if maritime frontal evolution can be generalized to a coastal environment.

The remainder of the thesis is organized as follows, Chapter II provides background information on rapid cyclogenesis, the ERICA project, current frontal models and a description of the NORAPS model. Chapter III presents a

synoptic discussion of the mesoscale frontal evolution of the IOP-5A cyclone as well as model verification through comparisons with actual observations. The final chapter contains conclusions and recommendations.

II. BACKGROUND

A. REVIEW OF CYCLOGENESIS

Sanders and Gyakum (1980) define an explosively developing extratropical cyclone as one in which the central pressure fall averages at least one mb h⁻¹ for 24 hours. In a northern hemispheric climatological study (for the period September 1976 to May 1979), Sanders and Gyakum (1980) found that these cyclones are primarily a maritime cold season event that usually occur downstream of a mobile 500 mb trough within or poleward of the maximum westerlies and within or ahead of planetary-scale troughs. Furthermore, these storms occur most frequently at the western portion of the North Atlantic and Pacific storm tracks near regions of strongest SST gradients.

Wash et al. (1988) note that there is a growing consensus that both upper-level and lower-level processes must work in concert for rapid cyclogenesis to occur. This philosophy is echoed by Uccellini (1990) who describes the upper- and lower-level features that are common to rapidly developing cyclones. Some of these common features include: (1) jet streak induced circulations with emphasis on the circulation pattern in the entrance/exit regions of the jets; (2) extrusion of stratospheric, high potential vorticity (PV) into the upper

and middle troposphere; (3) advection of absolute vorticity by the thermal wind particularly at the 500 mb level; (4) the thermal advection pattern in the lower troposphere in conjunction with the presence of low-level baroclinic zones and strong low-level winds; (5) sensible and latent heat fluxes in the boundary layer (especially over the ocean); (6) the decrease of the static stability in the lower troposphere related, in part, to the boundary-layer heating noted above; and (7) orographic effects. Uccellini (1990) hypothesizes further that these individual processes may be necessary but not sufficient to cause rapid cyclogenesis and that nonlinear effects may be important. In general, a high degree of variability between storms and the manner in which individual processes interact appears to be the key to rapid cyclogenesis.

Finally, Wash et al. (1992) found that there are significant differences in the initial conditions for explosive and nonexplosively deepening storms. The explosive developing storms display stronger upper-level divergence, stronger positive vorticity and a more vigorous upward vertical motion at the initial development time. In addition they also found that the presence of an upper-level source of divergence properly phased with the low-level incipient system was crucial for further rapid development.

B. ASPECTS OF THE EXPERIMENT ON RAPIDLY INTENSIFYING CYCLONES OVER THE ATLANTIC (ERICA)

The ERICA field study was designed to study rapid cyclogenesis and collect data over the northeastern United States and southeastern Canadian coasts, a known region for rapid cyclogenesis events. Hadlock and Kreitzberg (1988) identified three specific objectives of the program,

"... (1) understand the fundamental physical processes occurring in the atmosphere during rapid intensification of cyclones at sea, (2) determine those physical processes that need to be incorporated into dynamical prediction models through efficient parameterizations if necessary and (3) identify measurable precursors that must be incorporated into the initial analysis for accurate and detailed operational model predictions."

The field phase of ERICA was conducted from 1 December 1988 to 26 February 1989, and involved several agencies and collection platforms. To meet the goals of the experiment, the field study utilized research aircraft from the U.S. Navy, U.S. Air Force, the National Center for Atmospheric Research (NCAR), and the National Oceanic and Atmospheric Agency (NOAA). Other special data included: moored and air-deployed drifting buoys, coastal marine stations, ships of opportunity and supplemental rawinsondes. The conventional, operational meteorological systems routinely employed by the United States and Canada were also used.

During the field study, a total of nine Intensive Observation Periods (IOP's) were conducted. The criteria for an IOP was that a cyclone intensification of at least ten mb

$(6 \text{ h})^{-1}$ for at least six hours was expected within the ERICA domain.

C. MESOSCALE FRONTAL STRUCTURE OF CYCLONES

The Norwegian cyclone model developed by Bjerknes and Solberg (1922) has provided a conceptual understanding of the evolution of frontal systems associated with extratropical cyclones. At the time this theory was developed, Bjerknes did not have technological resources nor a detailed upper-air data collection network to support his conclusions. As technology and data collection have advanced, so to has the theory of frontal development.

Detailed ERICA observational studies, and realistic numerical simulations led Shapiro and Keyser (1990) to pose a new conceptual model, which describes four phases of frontal structure during the life of an extratropical cyclone (Figure 1). The four phases are,

"... 1) the continuous and broad front which represent the birthplace of the incipient frontal cyclone; 2) the frontal fracture in the vicinity of the cyclone center and scale contraction of the discontinuous warm and cold frontal gradients; 3) the frontal T-bone and bent-back warm front, characteristic of the midpoint of cyclogenesis; and 4) the warm-core seclusion within the post-cold frontal polar air stream representing the culmination of frontal evolution with the mature fully developed cyclone."

This conceptualization by Shapiro and Keyser (1990) has been verified by observation on two occasions, and has been reproduced in numerical model simulations. One observational

case occurred in the central Pacific on 8-10 March 1987, and is discussed by Shapiro and Keyser (1990). An example of the frontal fracture and the T-bone phase was also observed during a pre-ERICA test flight on 27 January 1988. The details of that study are discussed by Neiman et al. (1990). Both observed situations were located in marine environments. Neiman and Shapiro (1993) also observed the four phases of frontal development during ERICA IOP-4 cyclone which occurred between 4 and 5 January 1989. They found frontal features consistent with their conceptual model extended upward to 500 mb and were most pronounced at the 850 mb level.

Presently, it is not known whether this frontal hypothesis can be generalized to other (non-marine) types of storms. For instance, in contrast to Shapiro and Keyser (1990), Mass and Shultz (1993) found that the surface frontal system evolved into a classical occlusion pattern similar to that associated with the Norwegian cyclone model in a simulation of rapidly developing cyclone over land. However, the 800 mb thermal field suggested a bent-back warm front and weaker cold front as in the T-bone model. Mass and Shultz speculated that the difference between their results and those of Shapiro and Keyser (1990) could be attributed to the difference between the surface friction properties of the land and the ocean. One objective of this thesis is to determine whether the Shapiro and Keyser frontal evolution existed during the rapidly deepening ERICA IOP-5A coastal cyclone.

D. THE NAVY OPERATIONAL REGIONAL ATMOSPHERIC PREDICTION SYSTEM (NORAPS)

In order to provide more accurate short term (36-48 h) forecasts for given regions of the globe, the Naval Environmental Prediction and Research Facility (NEPERF) developed the Navy Operational Regional Atmospheric Prediction System (NORAPS). The NORAPS model was designed to be globally relocatable, with a choice of either a Mercator, Lambert conformal or a polar stereographic grid. The grid spacing in both the horizontal and vertical as well as the number of grid points to be used can be altered to any desired level. A detailed description of the operational model is contained in Hodur (1982) and Hodur (1987).

For this study, a research version of NORAPS was used. This version contains several modifications to the operational model. The hydrostatic primitive equations are solved on an Arakawa-C grid with a sigma vertical coordinate. Advection is handled using fourth-order finite differencing. Boundary conditions are taken from the U.S. Navy Operational Global Atmospheric Prediction System (NOGAPS) at six hour intervals. The analysis portion of NORAPS performs a multi-variate optimum interpolation analysis on 16 standard pressure levels every six hours using (NOGAPS) as the first guess. The horizontal domain consists of a 109 x 82 grid point array centered at 45⁰N, 65⁰W. The horizontal resolution is 60 km and the model is run with a 40 second explicit time step. Terrain

is obtained from the U.S. Navy ten minute data base. Additional details on the NORAPS analysis method used in this study are provided in Hirschberg and Langland (1992).

III. FRONTAL EVOLUTION OF ERICA IOP-5A

The time period 18-22 January 1989 was one of the more interesting of the ERICA project. During this five day period, two rapidly intensifying cyclones developed within 36 h over the western North Atlantic Ocean. The first cyclone, IOP-5, developed off the mid-Atlantic coast and tracked along the north wall of the Gulf Stream, reaching a maximum deepening rate of 18 mb (6 h)^{-1} (Hadlock et al. 1989). The second cyclone, IOP-5A, developed northeast of Lake Ontario and tracked along the Canadian Maritimes coast, reaching a maximum deepening rate of 15 mb (6 h)^{-1} .

This later storm is of particular significance because it is a coastal developing storm which combines rapid deepening over land as described by Mass and Shultz (1993) and also characteristics of marine development summarized by Shapiro and Keyser (1990).

Spinelli (1992) conducted a synoptic investigation of IOP-5A and determined several factors that contributed to the rapid development of the cyclone. Those factors were: 1) significant lower tropospheric thermal advection preceding the rapid intensification; 2) favorable superposition of a mobile 500 mb trough over the frontal wave providing upper-level support; 3) the presence of a jet streak on the eastern side of the 300 mb trough and; 4) intense upward vertical motions

within the frontal cloud band of the cyclone. In addition, an evaluation of the NORAPS model forecast against the NORAPS model analysis was conducted to determine the effectiveness of the model in accurately simulating a rapidly developing coastal cyclone. Spinelli (1992) concluded:

"On the synoptic scale, the NORAPS model forecasts produced a realistic simulation of the rapid cyclogenesis event. The important large-scale features such as location and intensity of the 500 and 300 mb troughs, vorticity centers, jet streaks and upper-level divergence areas were represented well. Thus, the model forecasts of the IOP-5A cyclone's position and intensity were relatively accurate."

Figure 2 depicts the track of the IOP-5A cyclone. The position and central pressure are presented for the forecast and analysis at six hour intervals. In this study, as in Spinelli (1992), the model initialization time was 1200 UTC 20 January 1989. Hereafter, time and date will be denoted as date/hour minute (e.g., 20/1200Z). The largest surface pressure error was an under forecast of five mb, which occurred during the rapid deepening phase. Forecast positions were very accurate with some error (forecast low northwest of the observed low) at the end of the development period (Figure 2). Table 1 from Spinelli (1992) further illustrates the excellent model performance.

In order to illustrate the model performance aloft, Figure 3 depicts the 500 mb forecast geopotential height forecast minus analysis height difference for the 24 h prognosis. At 21/1200Z there exists an open, short wave pattern, with a deep

trough extending from the Bay of Fundy along the U.S. east coast. The largest positive errors (only approximately 40 m) appear on the downstream side of the trough axis. Similarly, Figure 4 depicts the same fields at the 36 h forecast time valid at 22/0000Z. At this time, the forecast trough and closed low at 500 mb lagged the analysis by about 160 nm. Height errors in the vicinity of the upper-level trough are approximately 120 m, while errors over the rest of the domain are considerably less. The general success of NORAPS in forecasting the surface and upper-level features of this rapid developing coastal storm presents an opportunity to use the model data sets to study more detailed aspects of the IOP-5A development.

To study how the frontal structure evolves over time during IOP-5A, primary emphasis will be given to the sea level pressure charts combined with the surface thermal and wind fields. Similar fields for the 900 mb level will also be presented. Frontogenesis computations for the surface and 900 mb level will also be provided. Fields of frontogenesis were obtained using the Miller and Petterssen equation. The Lagrangian derivative of the horizontal potential temperature gradient, formed by applying the Euler expansion as found in Carlson (1991 p. 351), is shown below,

$$\frac{d}{dt} |\nabla_p \theta| = \nabla_p \theta^{-1} \left(- \left[\left(\frac{\partial \theta}{\partial x} \right)^2 \frac{\partial u}{\partial x} + \left(\frac{\partial \theta}{\partial y} \right)^2 \frac{\partial v}{\partial y} \right] - \left[\frac{\partial \theta}{\partial x} \frac{\partial \theta}{\partial y} \left(\frac{\partial v}{\partial x} + \frac{\partial u}{\partial y} \right) \right] \right)$$

$$\begin{aligned}
& - [(\frac{\partial \theta}{\partial x}) (\frac{\partial \theta}{\partial p}) \frac{\partial \omega}{\partial x} + (\frac{\partial \theta}{\partial y}) (\frac{\partial \theta}{\partial p}) \frac{\partial \omega}{\partial y}] \\
& + [\frac{\partial \theta}{\partial x} \frac{\partial}{\partial x} (\frac{d\theta}{dt}) + \frac{\partial \theta}{\partial y} \frac{\partial}{\partial y} (\frac{d\theta}{dt})] \quad (1).
\end{aligned}$$

For this study only the confluence and shear terms, the first two terms on the right side of equation, will be used to estimate $d/dt |\nabla_p \theta|$. The remaining terms were not found to be significant. The first sigma level of the NORAPS model (approximately 2 meters above the surface) was used to produce fields of surface frontogenesis. In addition, model vertical soundings will be evaluated and compared to actual soundings observed during the experiment. Model cross sections will also aid in determining frontal position and structure.

There remains significant interest in frontal evolution as noted in Neiman and Shapiro (1993), Mass and Shultz (1993), as well as McGinnigle (1988). In addition, forecasting the structure and development of sub-synoptic scale features in coastal areas remains a difficult task, largely because timely synoptic observations often end at the shore line. Even with special collection efforts such as the ERICA study, large ocean areas may not be adequately sampled, leaving large gaps where significant mesoscale activity may develop. In an effort to combat the sparsity of data, gridded data sets are often used in place of unverified analyses. Therefore, this study utilizes a data base consisting of the 3-hourly NORAPS forecast fields augmented with the special data available from

the ERICA studies. The ability of the high resolution model to resolve the sub-synoptic scale features and the frontal evolution of a rapidly deepening coastal cyclone will be established.

A. 20/1200Z January 1989

Figure 5 presents the sea-level pressure and isotherms at the start of the forecast period, 20/1200Z. At this time the incipient low is located north of Lake Ontario with a central pressure of 1003 mb. The IOP-5 cyclone is located 1,100 nm farther to the east with a central surface pressure of 980 mb.

A complex frontal pattern exists with four distinct baroclinic zones evident. An arctic front extends southwest from central Quebec, upstream of the low through Michigan, Illinois and ending in northeastern Missouri. This front is very intense north of the Great Lakes as evidenced by the tight temperature gradient. A northern warm frontal band extends from the low center, east through Quebec and into New Brunswick. The polar front extends south of the low along the pressure trough through western New York, central Pennsylvania, Virginia and across western North Carolina. This cold front is not clearly indicated in the isotherm analysis at this time but is evident in the isobar pattern and is carried on operational National Meteorological Center (NMC) charts (not shown). In addition, a coastal front is evident that extends from the New Jersey shore, southwest along the

east coast. A very weak warm front intersects the coastal front along the temperature ridge line and extends to the southeast. There is an open wave in the temperature pattern with a warm tongue along the Southeast Coast. This feature is also evident at 850 mb (Figure 6) and at levels up to 600 mb (not shown). The arctic front and polar front are also present at 850 mb as well.

B. 20/1800Z January 1989

Over the next six hours, the low center moves east and the central pressure deepens slightly to 1001 mb (Figure 7). By 20/1800Z, the northern portion of the arctic front extends across Quebec and Lake Ontario. The portion of the front southwest of Lake Ontario began to dissipate. A weak warm front is still evident north and east of the surface low. This warm front intersects the arctic front in southern Quebec and extends northeast across the mouth of the St. Lawrence River and into eastern Quebec. The cold synoptic (polar) front has pushed east and extends southwest from eastern Pennsylvania, to South Carolina. The thermal packing of this front is more clearly defined at this time. The coastal cold front and the associated warm front are notably stronger as well.

Figure 8 depicts surface frontogenesis at this time. Three areas of positive values, which directly correlate with the locations of the arctic, synoptic-scale cold, and the coastal fronts are evident. The outermost contour of the positive

areas have been highlighted for ease of identification. The arctic front displays the largest frontogenesis values at this time. Figure 9 depicts model surface latent heat fluxes. The areas of maximum latent heat flux just off the East Coast correspond with the general position of the Gulf Stream. Another latent heat maximum near 40°N , 50°W is located to the southwest of the IOP-5 center. Significant dewpoint depressions (Figure 9) over the open ocean indicate surface latent heat fluxes are occurring as indicated by the model. The distinct appearance of dual fronts along the East Coast is not observed in the thermal pattern at the 900 mb level, (Figure 10). However, a broad baroclinic zone can be seen from New England and eastern Canada to the southeastern United States. In addition, the intense arctic front is evident over Quebec west of the low.

A developing cloud wave pattern can be seen in the GOES satellite imagery of 20/1801Z (Figure 11). The darkest enhanced cloud tops in the upper right half of the image are associated with IOP-5. There are three distinct cold (enhanced) cloud regions over eastern Canada and the U.S. east coast. The southernmost cloud tier is associated with the coastal front and also corresponds closely to the areas of maximum surface latent heat flux as shown in Figure 9. The middle and northern tiers are associated with the arctic front and the incipient surface system.

The NORAPS forecast fields and satellite data illustrate the complexities of the IOP-5A cyclone structure early in its development. Specifically, this cyclone does not form along a single, baroclinic zone as discussed by Neiman and Shapiro (Figure 1) or by Mass and Shultz (1993). In particular, the cloud and frontal analysis show several important pre-existing baroclinic zones on the edge of the developing cyclonic circulation. An intensifying coastal front with a distinct warm tongue to the south and a strong arctic front present west of the low. The circulations associated with these fronts appear responsible in organizing the significant clouds and precipitation as depicted in Figure 11.

C. 21/0000Z January 1989

By 21/0000Z, the synoptic-scale low moves to the southeast and is positioned over central Maine with a pressure of 997 mb (Figure 12). The mesoscale details associated with this movement will be discussed shortly. Rapid deepening of the storm is now beginning to occur. The arctic front has moved east as well, and is located just west of the low. A small warm frontal boundary persists over southern Quebec. Over the past six hours the synoptic cold front weakened and likely merged with the coastal front, which intensified over the western Atlantic Ocean. Since the coastal front has moved with the developing system away from the coast, it will be referred to as the synoptic cold front hereafter. The synoptic warm

frontal boundary associated with this cold front can clearly be seen in the isotherm field (Figure 12) and on the surface frontogenesis chart as a separate area of positive frontogenesis (Figure 13). The surface frontogenesis also shows that the arctic front is intensifying, and extends farther to the northeast into the Gulf of St. Lawrence. The arctic frontogenesis is due to convergence associated with cyclone circulation.

An examination of the 900 mb temperature forecast (Figure 14), shows that a distinct rotation of the thermal ridge over New England from a southwest-northeast orientation to a more north-south alignment had occurred over the last six hours. Rotation of the thermal ridge is not evident at the surface however. The presence of the warm tongue has become more evident as can be seen by the 8°C contour line, which now extends north of 40°N .

Frontal areas are also evident on GOES infrared satellite imagery valid at 21/0001Z (Figure 15). There is a distinct frontal wave cloud signature associated with the old coastal and warm front south of Maine. In fact, the coldest cloud tops ($< -60^{\circ}\text{C}$, the dark enhanced areas of the image) are located near the peak of the warm sector. The most intense areas of the polar front can be located by the enhanced cloud area extending from Maine to eastern Canada.

D. 21/0300Z January 1989

Over the next three hours the IOP-5A cyclone tracks east and is centered over eastern Maine with a central pressure of 993 mb (Figure 16). The arctic front has moved east and once again is evident as far south as eastern West Virginia. Very cold continental arctic air is located northwest of the front over Ontario. The northern warm front is still evident in southeastern Quebec. The synoptic cold front has moved east and the warm front has rotated slightly to the north. The two separate areas of surface frontogenesis associated with the coastal front six hours earlier (Figure 13) have merged into a more intense single area (Figure 17). Strong frontogenesis continues along the arctic front west of the cyclone.

The 900 mb isotherm pattern southeast of the surface low (Figure 18) resembles a bent-back warm front configuration similar to the Shapiro and Keyser (1990) model. The first significant evidence of frontogenesis at the 900 mb level is evident (Figure 19) and is nearly identical to that found at the surface (Figure 17). Significant frontogenesis of the arctic front is also present at 900 mb appearing as two distinct centers over Maine and eastern Canada.

E. 21/0600Z January 1989

Over the next three hours the low continues to track along the northern coast of the Bay of Fundy and deepens another four mb to 989 mb (Figure 20). The arctic front has moved

significantly to the east over the Gulf of St. Lawrence to New England following the movement of the surface low. The northern warm front is clearly defined bending south from southern Quebec to St. Georges, Newfoundland. The synoptic cold front continues to move east and the associated warm front rotates slightly to the north. Surface latent heat flux computed by NORAPS continues to show a maximum value in the vicinity of the Gulf Stream with a secondary maximum immediately downstream of the coastal front in the area of the warm sector (Figure 21). Again, dewpoint depressions are shown in the figure from the observed surface reports. An increase of the surface fluxes from 20/18Z (Figure 9) is consistent with larger dewpoint depressions than at 21/06Z.

Cold-air advection northwest of the surface low continues to amplify the bent-back appearance of the isotherms at the 900 mb level (Figure 22). The thermal ridge, north of 44°N shifted to a more southeast to northwest orientation due to the circulation about the cyclone. Figure 23 which depicts frontogenesis for the 900 mb level, shows greater values compared to the surface. Also present is the distinct formation of a warm frontal zone that is perpendicular to the main cold front. The polar front appearance and development of a distinct warm frontal band are also evident in the 850 mb fields (not shown).

GOES satellite imagery valid at 21/0601Z (Figure 24) shows two distinct cloud mass structures. The cloud mass with the

darkest (coldest) tops is located to the southeast of the low center and is associated with the synoptic fronts. The second major cloud mass located over eastern Quebec has formed in the cold polar air upstream of the old coastal front, and shows comma cloud characteristics. The satellite imagery agrees with model frontal forecasts showing the merger of the pre-existing fronts during the cyclogenesis period.

F. 21/1200Z January 1989

After 21/06Z, the IOP-5A cyclone moves from the Bay of Fundy, near Saint Johns, to a position on the eastern shore of Prince Edward Island. A deepening rate of $13 \text{ mb } (6 \text{ h})^{-1}$ is indicated in the NORAPS forecast from 21/0600Z to 21/1200Z, and the central pressure drops to 978 mb (Figure 25).

The arctic front continues to intensify and move to the east. However, between central Labrador and the western Gulf of St. Lawrence, the front has moved westward approximately 30 nm over the past six hours due to the circulation about the cyclone. Although the northern warm front remains in the same location, it's intensity is weaker. The synoptic frontal system continues rotating cyclonically but now extends to the cyclone center where it intersects the arctic front. This section of the synoptic front, between the arctic front and the triple point, is classified as a warm type occlusion because the coldest air mass is located ahead of the front. The surface temperature field immediately to the south of the

low center continues to show a cyclonic rotation of the thermal ridge. This rotation is similar to that which was seen 12 hours earlier (Figure 14) at the 900 mb level.

Surface frontogenesis values (Figure 26) have increased in three areas. Two are associated with the synoptic fronts and the third area with the arctic front. There is again a distinct separation between the cold and warm fronts of the synoptic baroclinic zone. Figure 27 shows the total accumulated precipitation for the previous six hours ending at 21/12Z. The general precipitation pattern closely follows the frontal pattern, while the local precipitation maximum is closely associated with the warm tongue from the south. A secondary maximum is found in the Gulf of St. Lawrence near the triple point of the arctic and northern warm front.

The 900 mb temperature pattern (Figure 28) shows that the arctic front has intensified during the past six hours with a marked cyclonic rotation of the cold front into the warm sector. The warm tongue from the south has narrowed and continues to extend into the low center. This thermal pattern is very similar to that found by Mass and Shultz (1993) with the cold front catching up to the warm front. Figure 29 depicts far more intense frontogenesis at the 900 mb level than is found at the surface.

Satellite imagery valid at 21/1201Z shows a distinct, mature comma head cloud with the largest cloud mass ahead of the low, over Newfoundland and a developing dry slot south of

the cyclone (Figure 30). The mature comma head cloud structure formed when a comma cloud in the polar air upstream of the main frontal band merged with the main cloud mass associated with the old coastal front. The cloud mass merging and evolution during the rapid deepening is very similar to the "instant occlusion" scenario described by Mullen (1983). The presence of the arctic front is indicated along a north-south line of the coldest (darkest) enhanced cloud tops. The synoptic fronts and associated warm tongue coincide with darkest cloud tops east of the dry slot. The cloud pattern seen in Figure 30 also closely corresponds to the precipitation depiction of Figure 27.

A vertical cross section from 43.3°N 68.8°W (in the cold air) northeast of the surface low to 48.2°N 51.5°W (south of the low and across the old coastal front and warm tongue) is presented in Figure 31. The location is indicated in Figure 25. The arctic front dominates the western side of the cross section extending nearly vertically from the surface to 900 mb and then bending westward to 800 mb. At the surface, the front is located over central Nova Scotia (Figure 25). The cross section bisects the warm tongue over Cabot Strait. The warm occluded front can be seen on the east side of the cross section. The model indicates saturated conditions above both the warm and the arctic fronts.

A sounding along the cross section at Yarmouth, Nova Scotia (WQI), verifies the location of the arctic front to be

between 850 mb to 800 mb (Figure 32). The model sounding for the same location positions the arctic front between 900 mb and 800 mb (Figure 33). Note the excellent agreement between the model and observed thermal structure. Both the observed and model soundings depict significant moisture values above and below the front. The model wind direction and speed correspond fairly well to the observed sounding. The model sounding however, depicts higher wind speeds at the jet level than was actually observed.

One other pair of model and observed soundings were compared. The location of these soundings is at St. Johns, Newfoundland (YYT), which is in the cold air east of the surface low position and on the east side of the cross section (Figure 31). The observed sounding (Figure 34) verifies the presence of the warm occluded front between 930 mb and 890 mb, while the model sounding (Figure 35) positions the warm front between 960 mb and 910 mb. Both soundings depict a shallow dry tongue between 940 mb to 800 mb, which is also evident on east side of the cross section (Figure 31). A deep moist layer is present above 800 mb in both the observed and model soundings. This layer is consistent with the deep vertically developed cloudiness east of the cyclone (Figure 30). These comparisons indicate the model skill at representing both the arctic front and frontal structure east of the cyclone at the 24 h point in the forecast.

G. 21/1800Z January 1989

The IOP-5A cyclone continued to deepen from 21/1200Z to 21/1800Z, but only at a rate of three mb $(6\text{ h})^{-1}$. During that time, the 971 mb center moved across the Gulf of Saint Lawrence at a speed of 25 kts (Spinelli 1992) to a position near St. Georges, Newfoundland (Figure 36). The frontal structure remained intact with the presence of arctic polar and synoptic fronts. The arctic front remains located on the west side of the low center in the general position of a bent-back warm front by the end of the period. The associated northern warm front has weakened and is no longer evident. The surface temperature structure shows that the elongated warm tongue has changed orientation to a nearly west-east alignment. The main cold front continued to intensify although there appears to be a weakening of the warm frontal region after 21/1200Z as depicted by the frontogenesis analysis (Figure 37). The bent-back structure at the 900 mb level continues to be more evident than at the surface (Figure 38). The largest frontogenesis values remain at the 900 mb level (not shown).

Satellite imagery at 1801Z (Figure 39) shows a mature cyclone vortex cloud pattern with the coldest cloud top temperatures ahead of the low, east of Newfoundland near the frontal triple-point location (Figure 36). The water vapor imagery valid at 1701Z (Figure 40) shows a very distinct dry slot extending from the Chesapeake Bay area, northeast to the

low center on the trailing side of the cloud band. A distinct hook of the moisture and clouds west of the cyclone is also evident in the vicinity of the surface low.

A vertical cross section from Bedford, Massachusetts (BED) 42.6°N, 71.1°W, through the surface low, crossing both the warm tongue and front and terminating in Gander, Newfoundland (YQX) 49.0°N, 54.8°W, is presented in Figure 41. The location of the cross section is shown in Figure 36. Two closed pools of arctic air below 900 mb dominate the west side of the cross section. The two cold pools are separated by the warming effect of the water where the cross section passes over the Gulf of Maine. The southern end of the arctic front is located near the center of the cross section where the tightest packed theta lines intersect the surface. The warm tongue in the isotherm patterns of Figures 36 and 38 is noted by the trough in the theta surfaces below 900 mb on the east side of the cross section. The dark (dry) area over central Newfoundland in the water vapor imagery mentioned above, coincides with the minimum in the relative humidity contours on the east side of the cross section above 600 mb. The relative humidity contours resemble the cloud pattern depicted in the warm and cold conveyor belt discussed by Carlson (1990 p.320). A dry slot (< 10% RH) extends down to 650 mb which separates very moist areas of the warm and cold conveyor belts. Below the dry slot high relative humidity values (90%) dominate near the surface.

The arctic front location is also evident in the observed sounding taken at Shearwater, Nova Scotia (YAW) as illustrated by the frontal inversions and deep moisture layer (Figure 42). The model sounding at this location also depicts a low-level inversion with high moisture values (Figure 43) again closely representing the actual sounding.

H. 21/2100Z January 1989

In the final stages of deepening the low moves northeast to a position in the Gulf of St Lawrence near St. Georges Bay and reaches its lowest forecast central pressure of 971 mb (Figure 44). The arctic front and the occluded front join west of Newfoundland in the northern portion of the low center. The occluded front has continued a counter-clockwise rotation about the vortex. A closed isotherm center has developed at the surface indicating the presence of a warm core seclusion similar to that described by Shapiro and Keyser (1990). Inspection of the 900 mb temperature chart (Figure 45) reveals the bent-back configuration of the thermal pattern is still more elongated and magnified than at the surface, however no seclusion is found at this level.

I. 22/0000Z January 1989

The final time period shows the IOP-5A cyclone maintaining a central pressure of 971 mb (Figure 46). The cyclonic rotation and northeast movement of the synoptic front

continues to suggest a frontal occlusion in the thermal pattern. In particular, the occluded front extends from just west of the low and wraps around the northwest side of the low center. The presence of a warm sector in conjunction with the synoptic cold front has become less distinct. The closed isotherm at the surface which is indicative of the warm core seclusion, has persisted and is located over Newfoundland.

The satellite imagery at 22/0001Z (not shown) shows a dissipating comma head with a front still visible. The main cloud band to the east of the low moved away from the cyclone center toward the east. The system, now fully mature and vertical begins to fill as it moves out over the North Atlantic Ocean.

J. Early Mesoscale Development

Spinelli (1992) conducted a subjective hourly analysis in order to more closely examine the mesoscale aspects of IOP-5A before the explosive deepening stage. From these analysis IOP-5A was found to have evolved from two separate low centers that the NORAPS analysis did not depict. Spinelli speculated that the secondary low, which developed on the east side of the Appalachian chain, resulted from lee side cyclogenesis and that this low deepened rapidly and likely became the primary low center for the IOP-5A system.

A subjective thermal analysis was performed on Spinelli's analysis of 1500Z/20 and is presented in Figure 47. The pre-

existing cyclone was located over southern Quebec with a central pressure of 1002 mb. The new secondary low was located approximately 150 nm to the southeast in southern Vermont with a central pressure of 1006 mb. The thermal pattern indicates that the northern low is centered on a weak thermal ridge with tight thermal packing occurring through the low center. A distinct warm tongue is analyzed from the south along the coast of Connecticut and New York to the southeast of the northern low. The warm tongue immediately precedes the synoptic cold front. A coastal baroclinic zone is analyzed to the east of the smaller low along the coast.

A subjective thermal analysis was also performed on Spinelli's analysis of 2100Z/20 and is presented in Figure 48. Over the previous six hours the tight thermal packing associated with the northern low center has weakened, while the leading edge of the polar front to the west appears to be intensifying. A warm tongue from the south extends well into the center of the secondary coastal low. A warm frontal band passes across the northern part of the low and a developing baroclinic zone can be seen to the west of the low. From 20/15Z to 21/21Z the northern low deepened 5 mb while the new coastal low deepened 8 mb.

The presence of a developing coastal baroclinic zone and tongue of warm air, which provides warm, moist, unstable air is conducive to further cyclone development. These factors

confirm Spinelli's speculation that the coastal low developed into the primary IOP-5A cyclone.

From the discussion above, the movement of the IOP-5A cyclone to the southeast, as noted in the 21/00Z synoptic discussion is consistent with the rapid deepening of the secondary coastal low. The failure of the NORAPS analysis and forecast to define a separate secondary low center may be due to resolution.

K. Summary

The frontal evolution of IOP-5A does not fit neatly into a single category of development. Rather, it showed properties similar to a classical occlusion and some evidence of the bent-back warm front structure as described by Shapiro and Keyser (1990).

An examination of the mature stage of the IOP-5A cyclone does show an intense frontal zone northeast to southwest of the low (Figure 36). This feature has been classified in other marine cyclones as a bent-back warm front (Shapiro and Keyser 1990). However, the cyclone shows a classic occlusion extending to the southeast of the storm (Figure 25). In addition, the evolution of these features is quite different than the other studies. In particular, pre-existing frontal zones intensified during the rapid cyclogenesis and evolved into cyclone frontal structures rather than forming as a result of the cyclogenesis.

A composite of the arctic front evolution is presented in Figure 49 at 12 hour intervals from 20/12Z to 22/00Z. The arctic front was a well defined baroclinic zone at the incipient stage of cyclone development. This front intensified as the cyclone developed and was consistently located in the immediate vicinity of the low throughout the observation period. The portion of the arctic front north of the cyclone, advanced ahead of the low, appearing to wrap around the cyclone. This forward advancement was only slowed during the most explosive deepening stage. The portion of the polar front south of the cyclone remained evident over land, but weakened as it crossed over the relatively warmer ocean waters. The associated warm front displayed a cyclonic rotation throughout development and finally weakened during the mature stage.

Figure 50 shows a composite of the coastal front positions every six hours from 20/12Z to 22/00Z. The coastal front began as a weak baroclinic zone along the Mid-Atlantic States, located well to the southeast of the incipient low. The front continued to rotate cyclonically and intensify, in the presence of a strong warm tongue, conveyor belt and developing low. The northern portion of the front occluded and extended into the low by 21/12Z.

Although there was supplemental observations from the ERICA project, there still is not enough surface marine and upper air data to study the sub-synoptic frontal structure of this coastal cyclone. Fortunately, the regional NORAPS

simulation provided a realistic depiction of the frontal features associated with this cyclone. Cross-sections and soundings from the model run were verified with available ERICA soundings. In addition, observed cloud features were in strong agreement with model diagnosed frontal circulations.

ERICA data was also used to determine the mesoscale features of the over-land coastal development period. A subjective thermal analysis revealed the presence of a warm tongue and a developing coastal baroclinic zone to the southeast of the new coastal low. The warm tongue provided elements that were conducive to secondary cyclone development. This thermal analysis supports the hypothesis that the mesoscale coastal low developed into the IOP-5A cyclone.

IV. CONCLUSIONS AND RECOMMENDATIONS

A. CONCLUSIONS

Analysis of the frontal evolution associated with the development of the cyclone observed during ERICA IOP-5A revealed that the frontal evolution was not a well-defined case of any single frontal evolution model. Distinct pre-existing fronts significantly influenced the frontal evolution throughout the observation period. The strong arctic and coastal fronts present at the incipient stage of cyclone development intensified as a result of the rapid cyclogenesis and became an integral part of the synoptic-scale frontal structure. An examination of the mature stage of IOP-5A did show intense frontal zones in areas similar to the bent-back warm front model presented by Shapiro and Keyser (1990), as well as a classic occlusion to Mass and Shultz (1993).

Comparisons of surface, upper air, satellite imagery leads to the conclusion that on the sub-synoptic scale, the NORAPS model provided a realistic depiction of the frontal location and intensities associated with this rapidly deepening coastal cyclone.

In order to resolve the over land mesoscale activity prior to the rapid deepening phase, manually produced subjective isotherm analyses were completed. A warm tongue and a coastal

baroclinic zone were analyzed in the vicinity of the new coastal low. These features provided elements that supported further cyclone development. The isotherm analyses reinforce the hypothesis that the new coastal low developed into the IOP-5A cyclone.

B. RECOMMENDATIONS

Examination of the frontal evolution of other ERICA storms is needed to determine the types of frontal evolution observed. In addition, the effect of pre-existing baroclinic zones on frontal evolution should also be evaluated.

The thermal analysis of this study supports the idea that the mesoscale coastal low developed into the primary IOP 5A cyclone; however, quantitative evidence to support that conclusion remains a research issue. Further studies to investigate the mesoscale coastal development stage are clearly needed.

The presence of the warm conveyor belt was noted in several places in this study however, it is not known how well this feature was modeled. The ERICA data set, and this storm in particular provides an excellent opportunity to determine the ability of the NORAPS model to accurately depict the structure of the warm and cold conveyor belts.

Finally, this study was primarily a qualitative overview of the IOP-5A frontal evolution. Future research efforts

should concentrate on performing more quantitative studies of the ERICA observational data and numerical model data.

APPENDIX

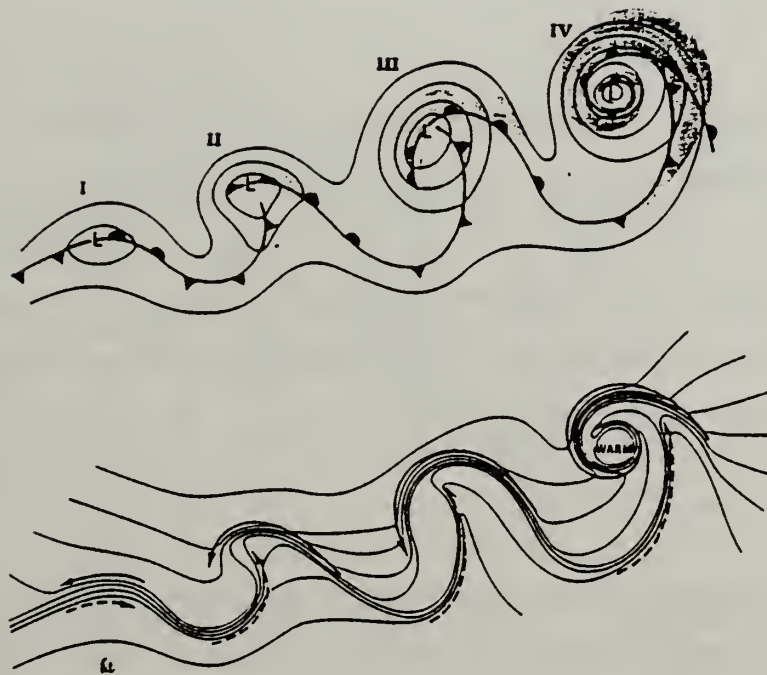


FIG. 10.27. The life cycle of the marine extratropical frontal cyclone: (I) incipient frontal cyclone; (II) frontal fracture; (III) bent-back warm front and frontal T-junction; (IV) warm-core frontal occlusion. Upper: sea-level pressure, solid lines; fronts, bold lines; and cloud signature, shaded. Lower: temperature, solid lines; cold and warm air currents, solid and dashed arrows, respectively.

Figure 1. Shapiro and Keyser (1990) Figure 10.27.

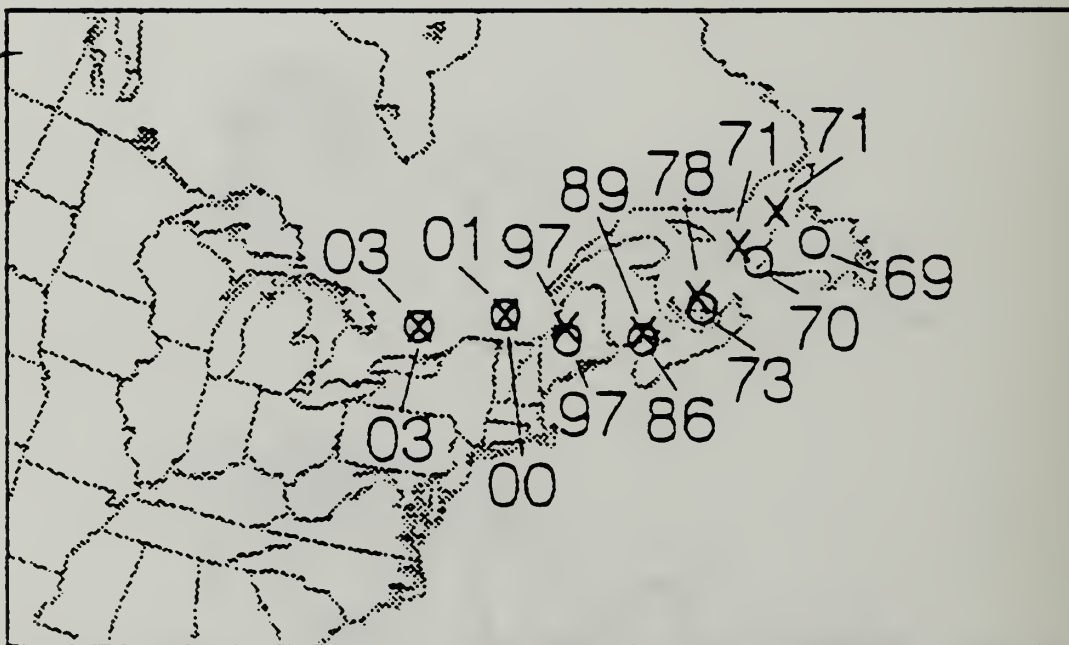


Figure 2. Track, (x's forecast position and pressure, o's analysis position and pressure) at six hour intervals from 20/12Z to 22/00Z.

Table 1. COMPARISON OF NORAPS FORECAST CENTRAL PRESSURE AND POSITION WITH ANALYSES FROM 1200/20 TO 0000/22 FROM SPINELLI (1992) .

| | analysis | forecast | pressure error | position error | direction |
|-------|----------|----------|----------------|----------------|-----------|
| 20/18 | 1003mb | 1003mb | 0 mb | 0 nm | none |
| 20/18 | 1000mb | 1000mb | + 2 mb | 0 nm | none |
| 21/00 | 997mb | 997mb | 0 mb | 0 nm | none |
| 21/06 | 986mb | 989mb | + 3 mb | 20 nm | north |
| 21/12 | 973mb | 973mb | + 5 mb | 60 nm | north |
| 21/18 | 973mb | 971mb | + 1 mb | 90 nm | northwest |
| 22/00 | 969mb | 971mb | + 2 mb | 160 nm | northwest |

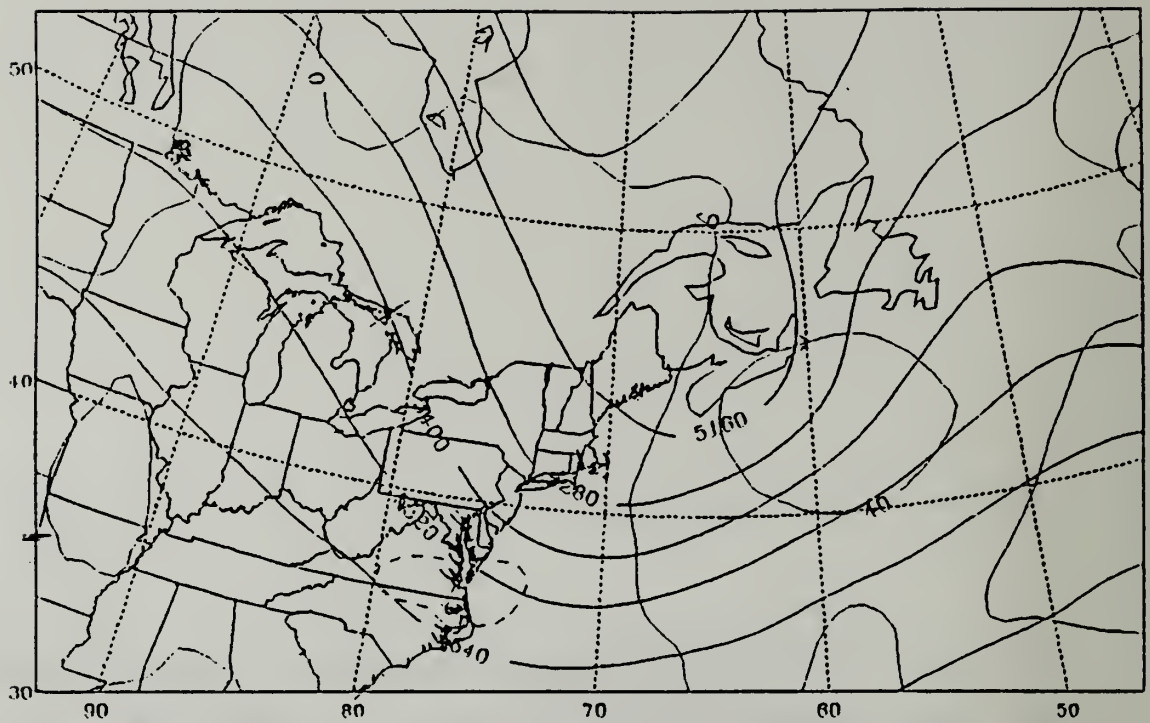


Figure 3. 500 mb height analysis (dark solid lines, contour interval 120 m) and forecast heights minus analysis heights (light lines, solid positive values, dashed lines negative values, contour interval 40 m) valid at 21/12Z Jan 1989.

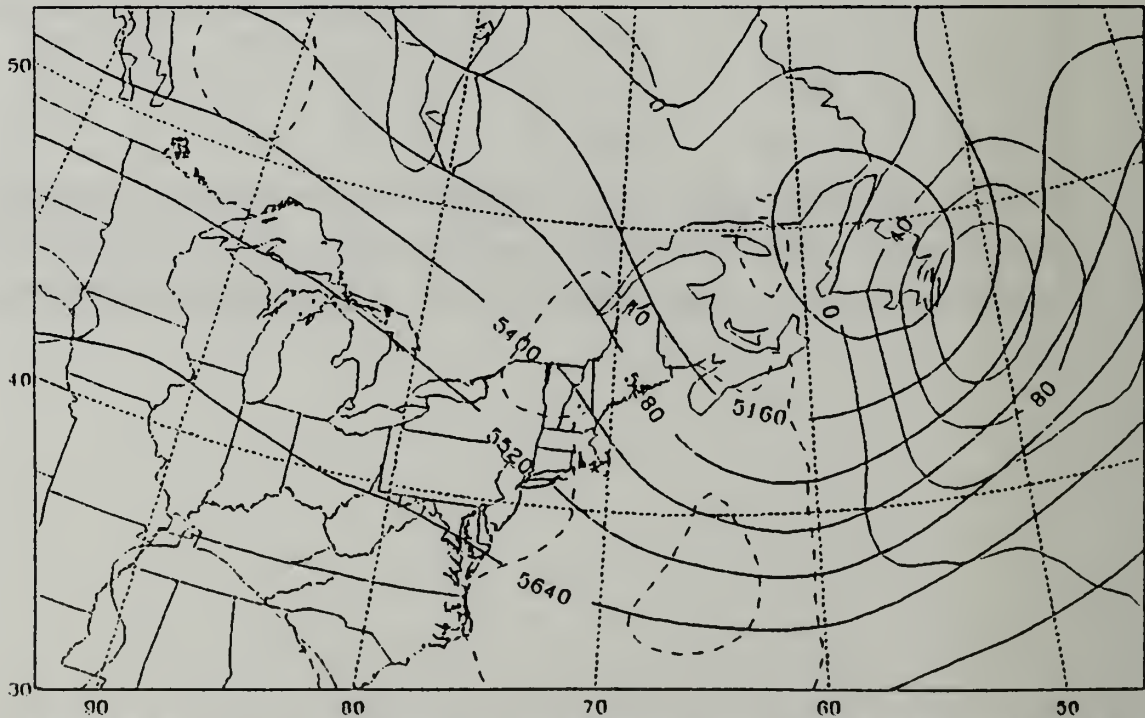


Figure 4. 500 mb height analysis and forecast heights minus analysis heights as in Figure 3, except for 22/00Z January 1989.

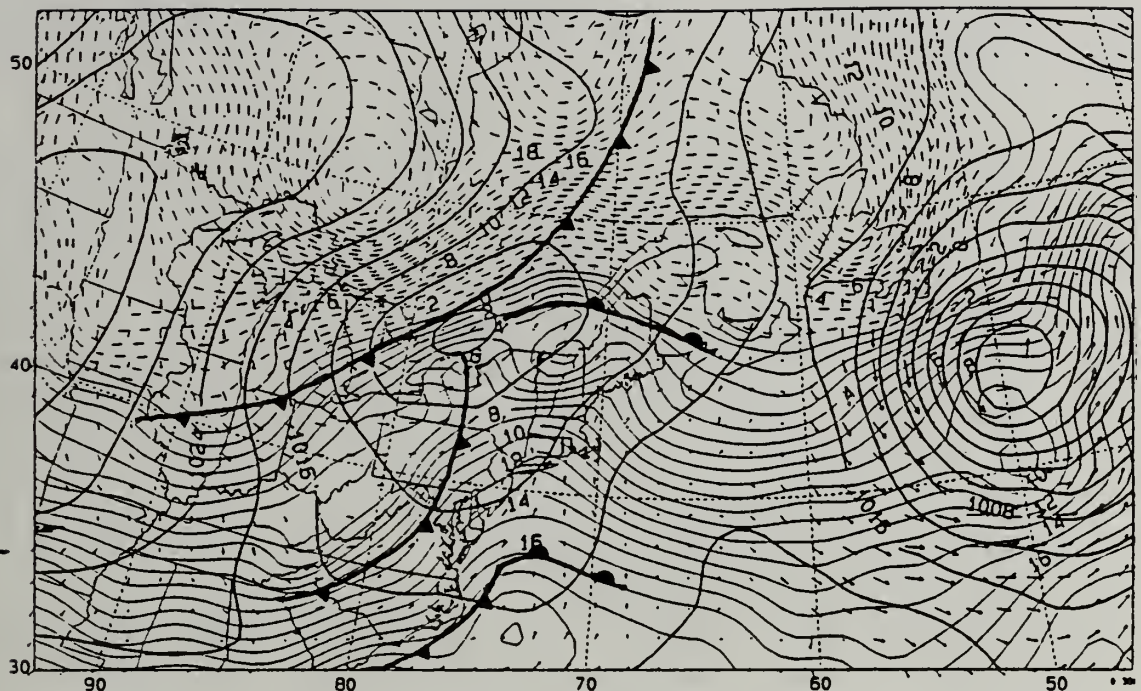


Figure 5. Sea level pressure (dark solid, contour interval 4 mb) and temperature (light solid, positive values, light dashed negative values, contour interval 1°C) valid at 20/12Z January 1989.

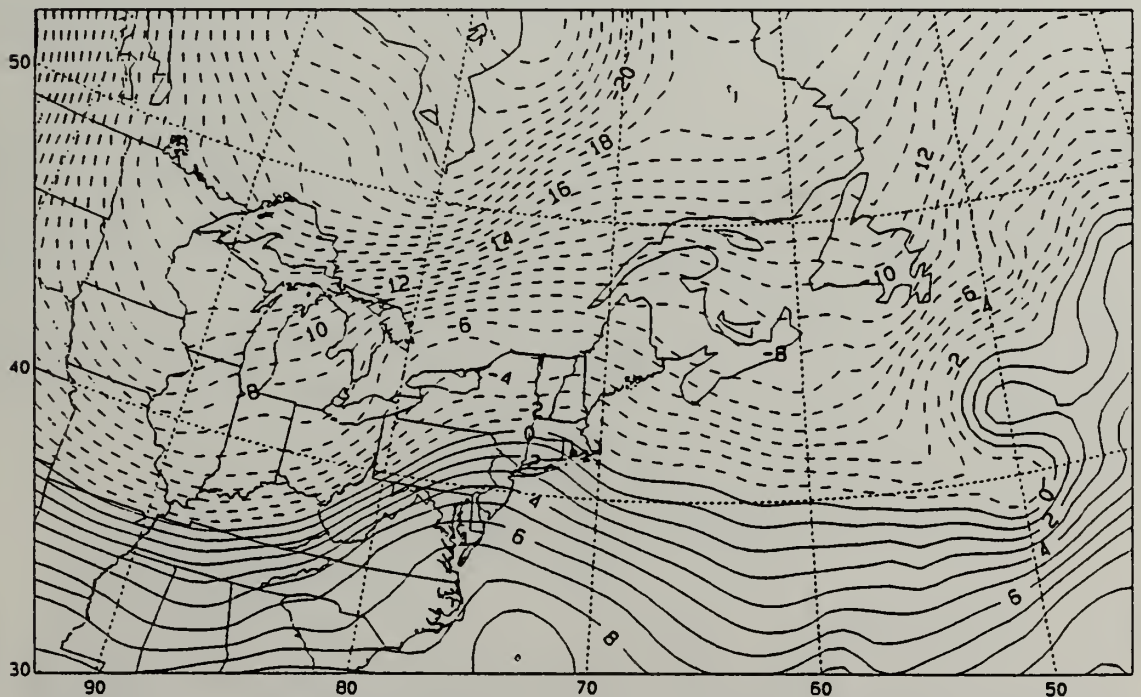


Figure 6. 850 mb temperature (solid, positive values, dashed, negative values, contour interval 1°C) valid at 20/12Z January 1989.

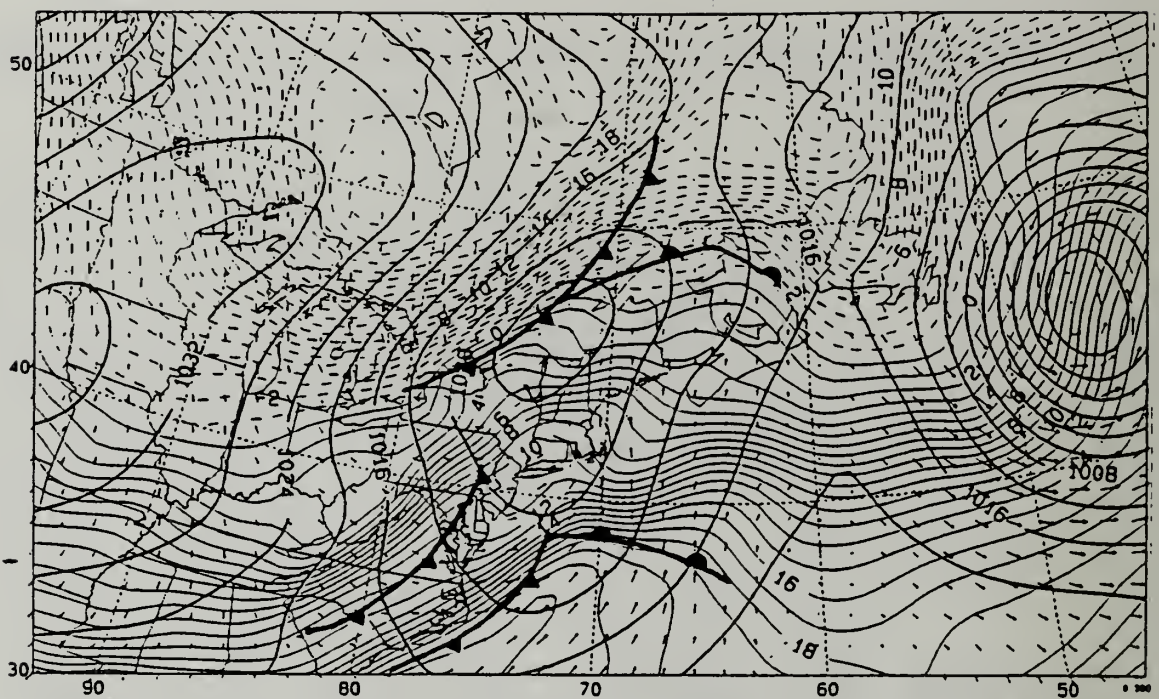


Figure 7. Sea level pressure and temperature as in Figure 5, except for forecast time 20/18Z January 1989.

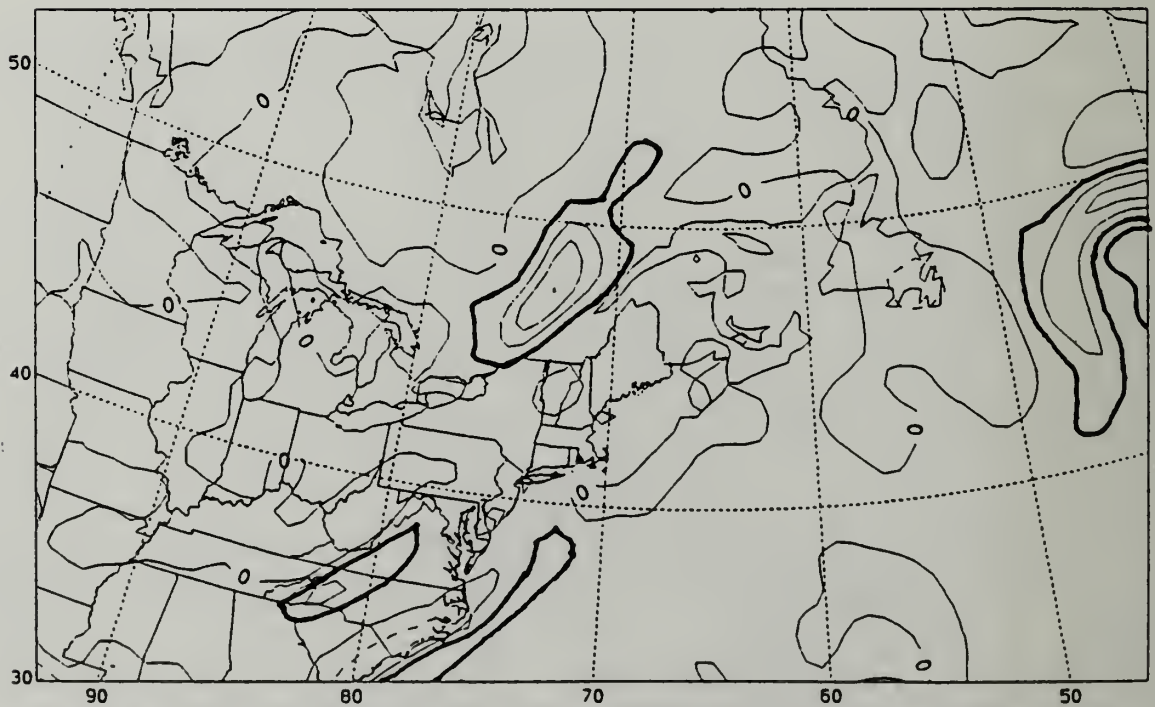


Figure 8. Surface frontogenesis (solid, positive values; dashed, negative values; contour interval $5^{\circ}\text{C}/\text{day}/100\text{ km}$) valid at 20/18Z January 1989.

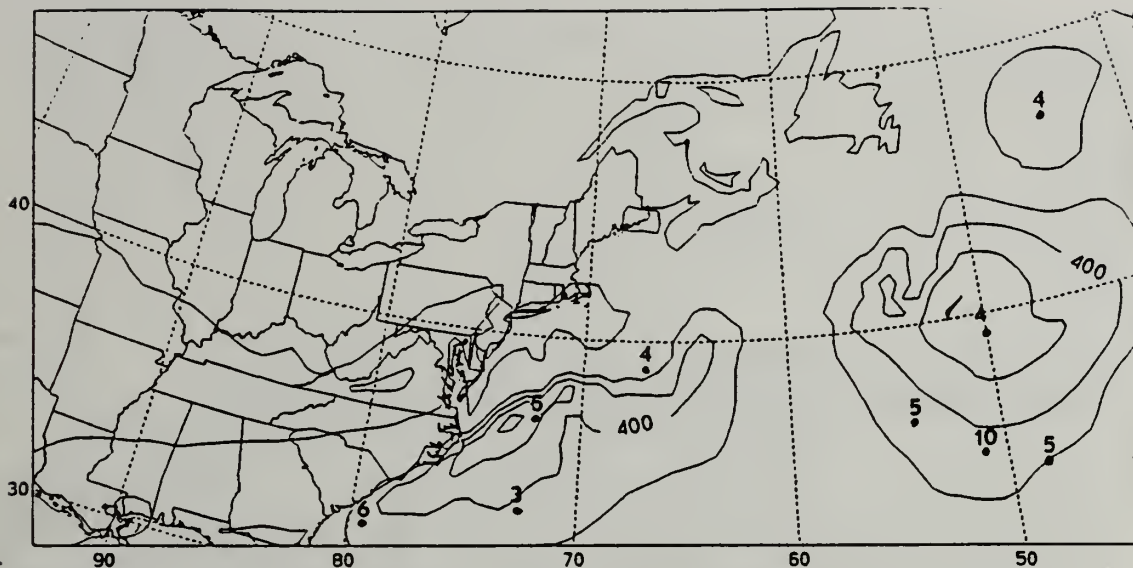


Figure 9. Surface latent heat flux, (contour interval 100 watts/ m^2) dots indicate surface report locations, numbers denote dewpoint depression, valid at 20/18Z January 1989.

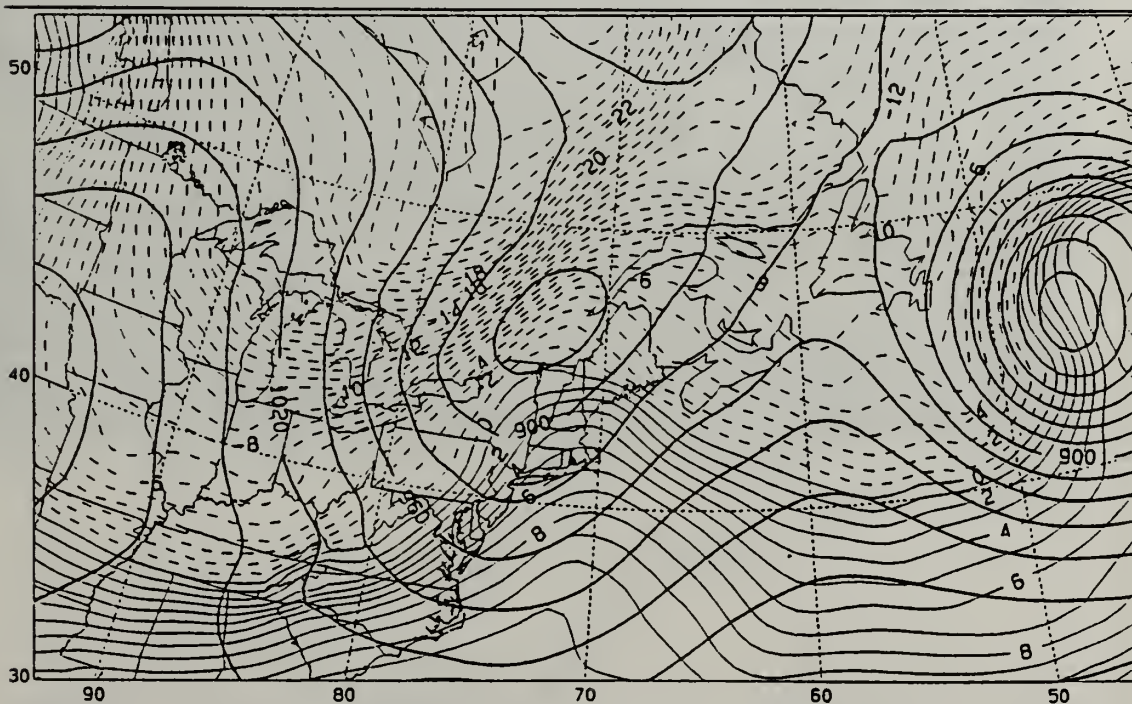


Figure 10. 900 mb geopotential height (dark solid, contour interval 30 m) and temperature (light solid, positive values, light dashed, negative values; contour interval 1 $^{\circ}$ C) valid at 20/18Z January 1989.

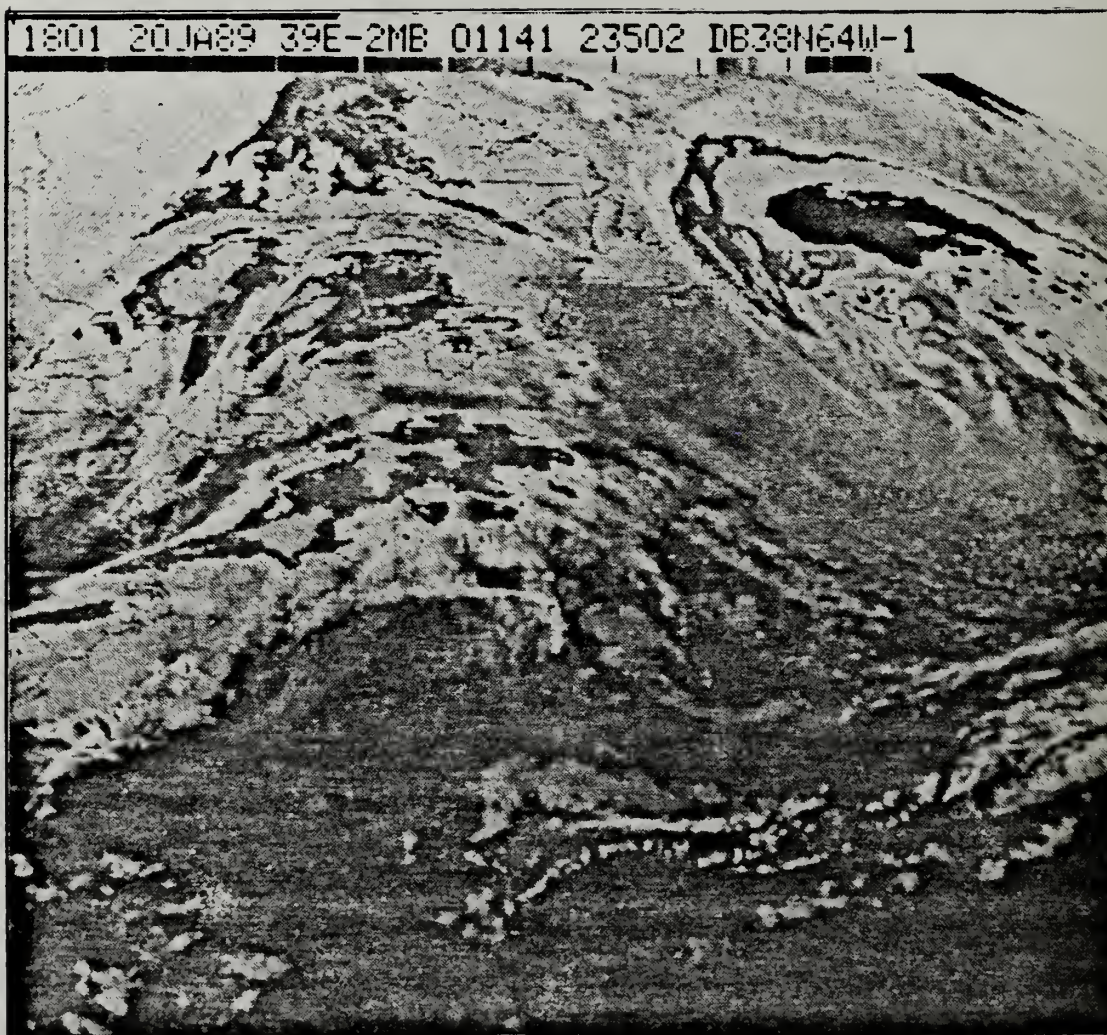


Figure 11. GOES enhanced IR satellite imagery at 20/1801Z January 1989.

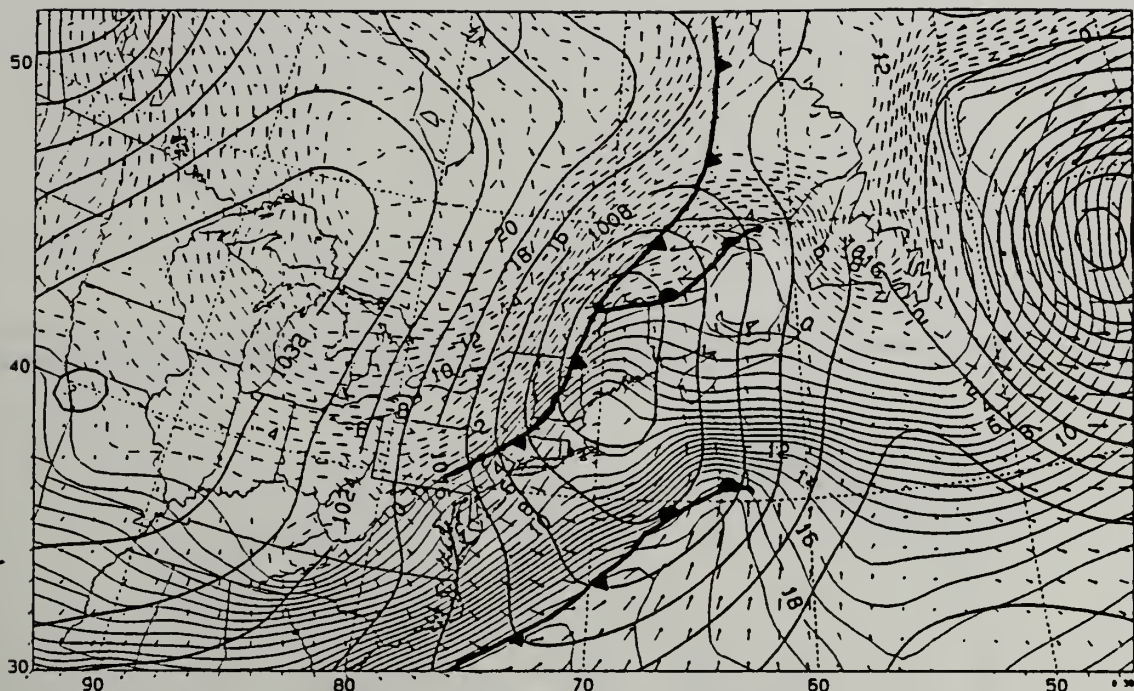


Figure 12. Sea level pressure and temperature as in Figure 5, except for 21/00Z January 1989.

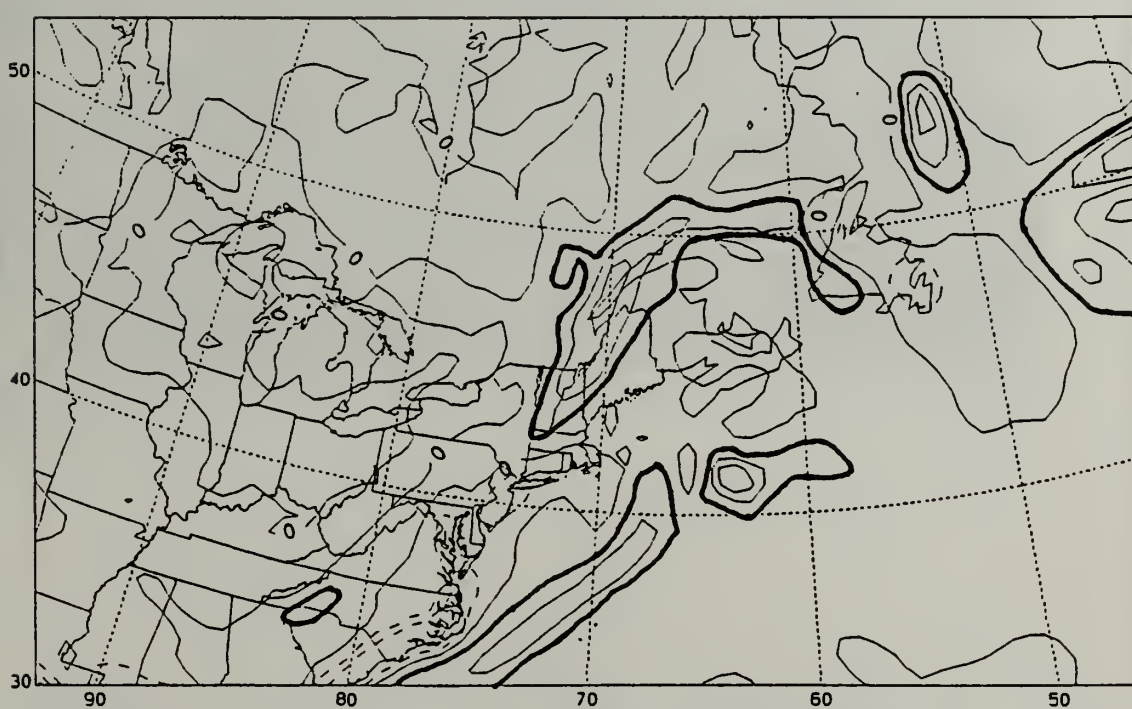


Figure 13. Surface frontogenesis as in Figure 8, except for 21/00Z January 1989.

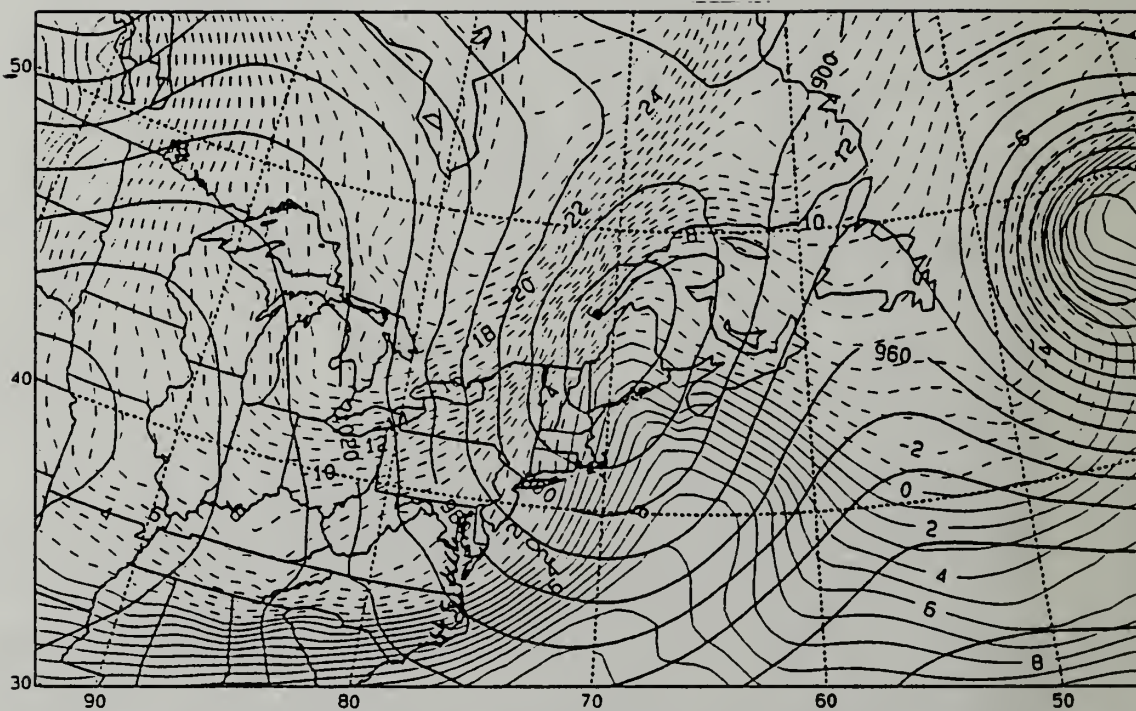


Figure 14. 900 mb geopotential height and temperature as in Figure 10, except 21/00Z January 1989.

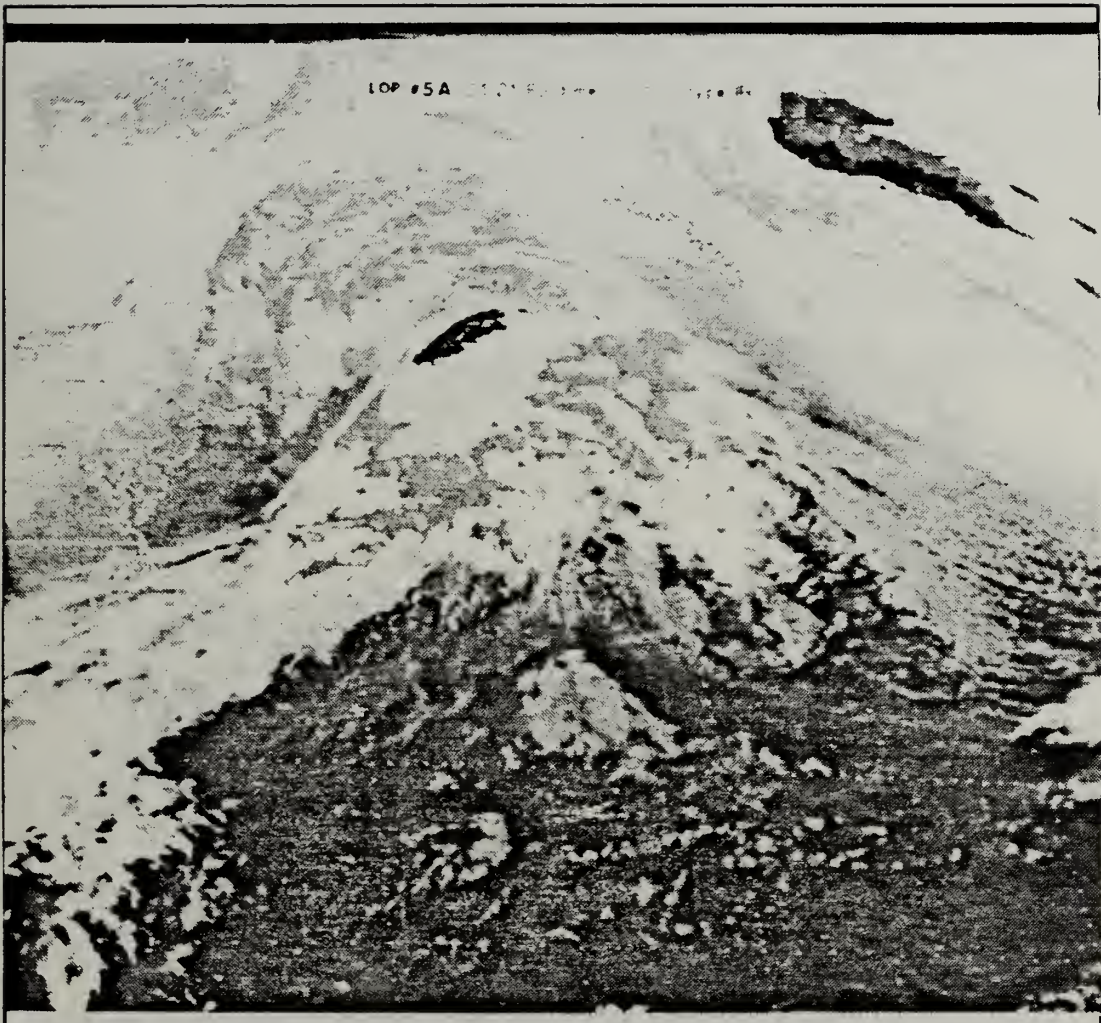


Figure 15. GOES enhanced IR satellite imagery at 21/0001Z January 1989.

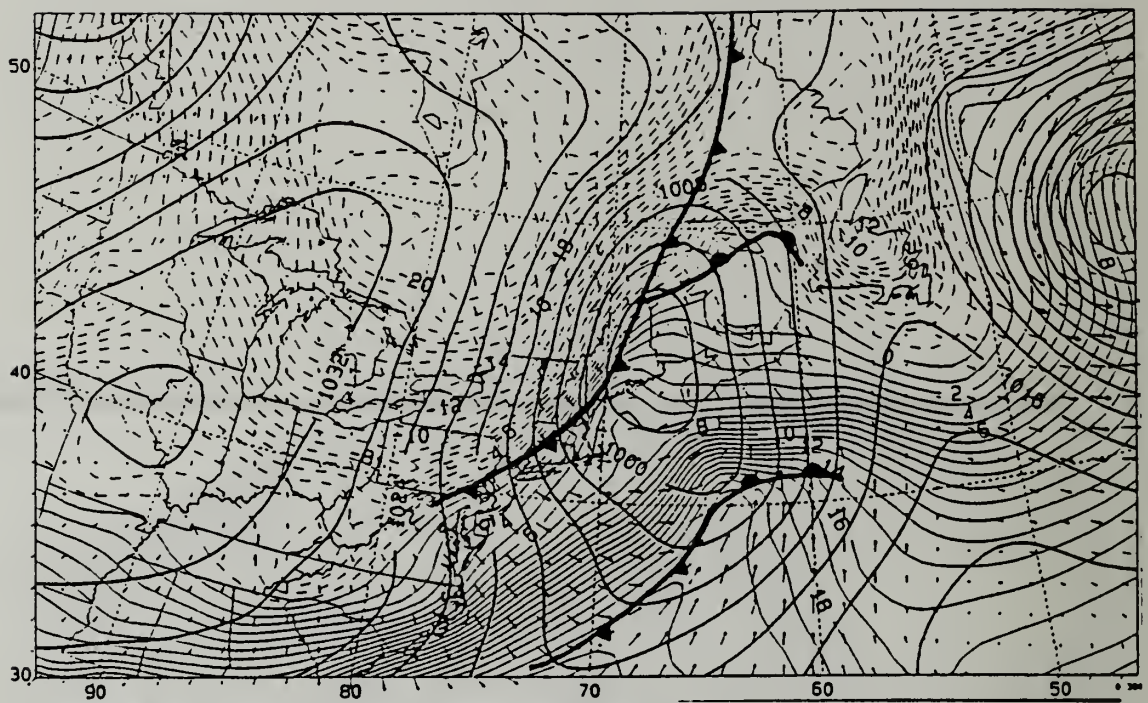


Figure 16. Sea level pressure and temperature as in Figure 5, except 21/03Z January 1989.

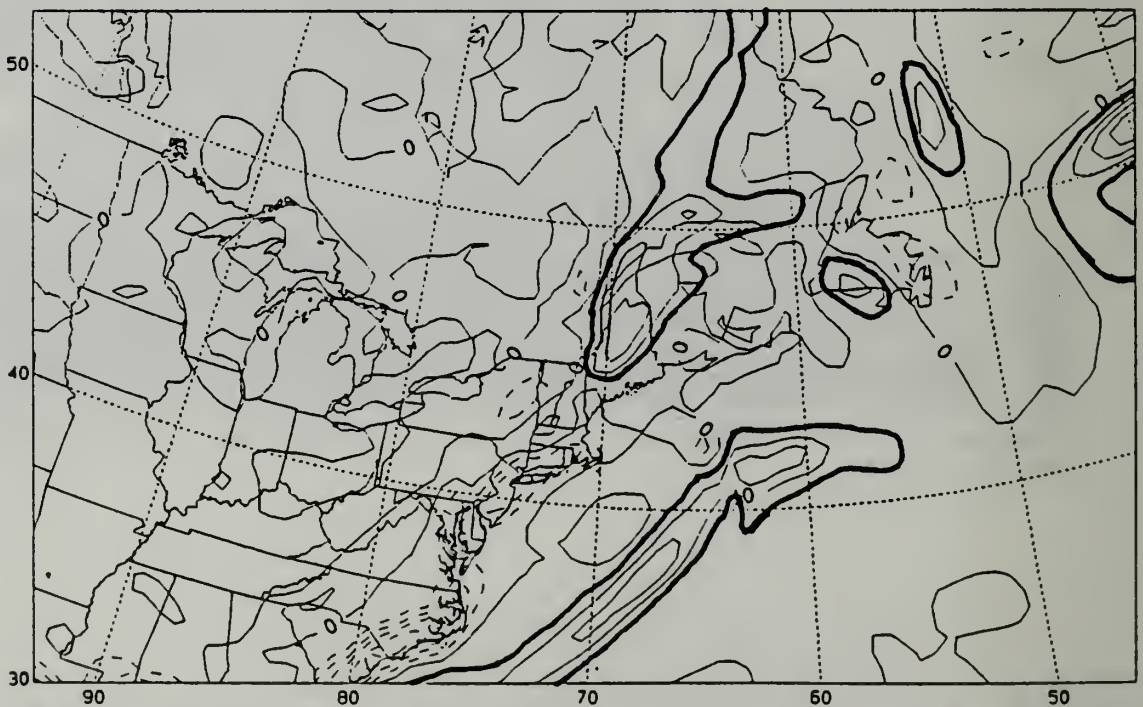


Figure 17. Surface frontogenesis as in Figure 8, except 21/03Z January 1989.

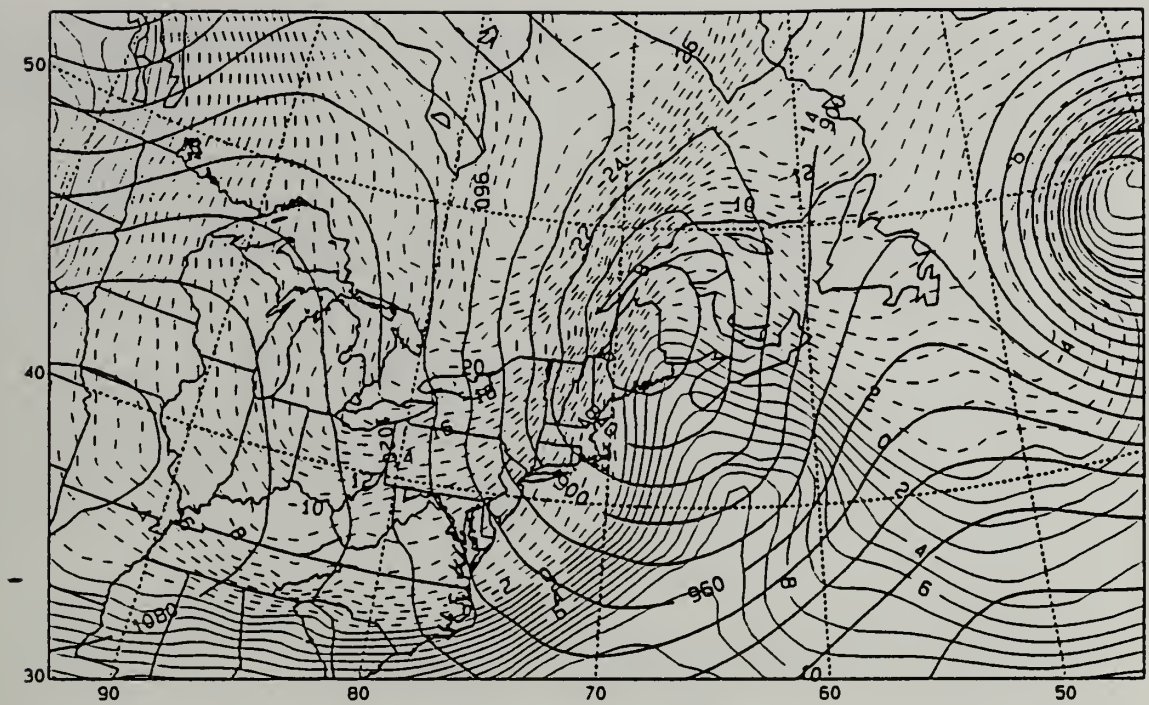


Figure 18. 900 mb geopotential height and temperature as in Figure 10, except 21/03Z January 1989.

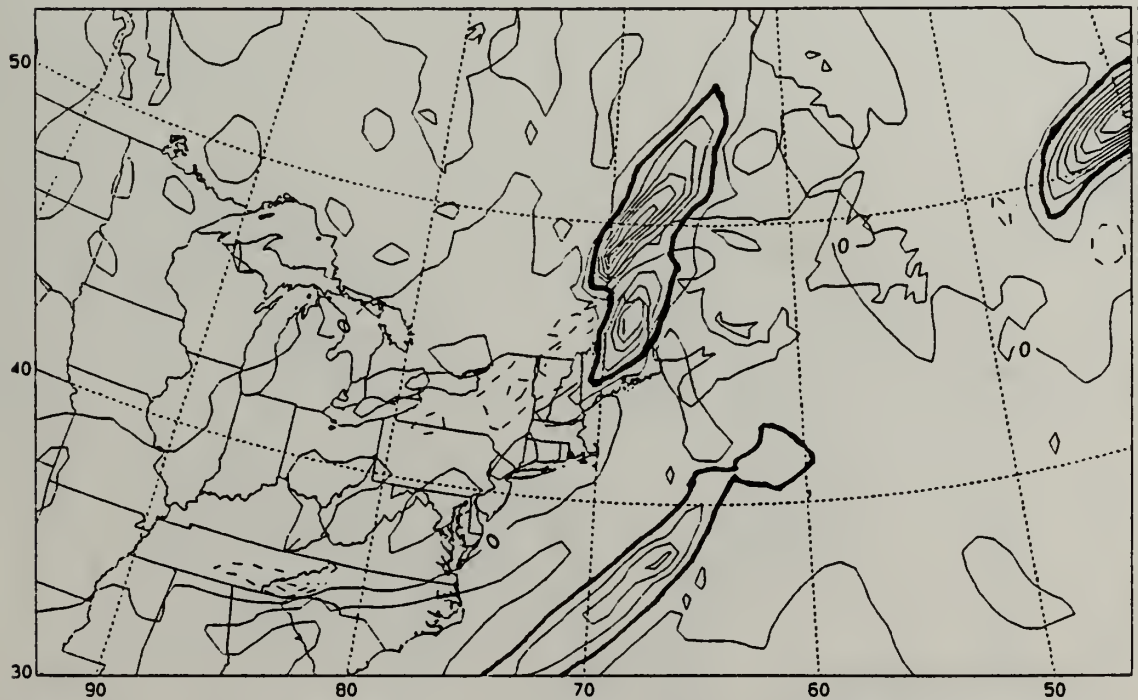


Figure 19. 900 mb frontogenesis (solid, positive values; dashed, negative values; contour interval $5^{\circ}\text{C/day/100 km}$) valid at 21/03Z January 1989.

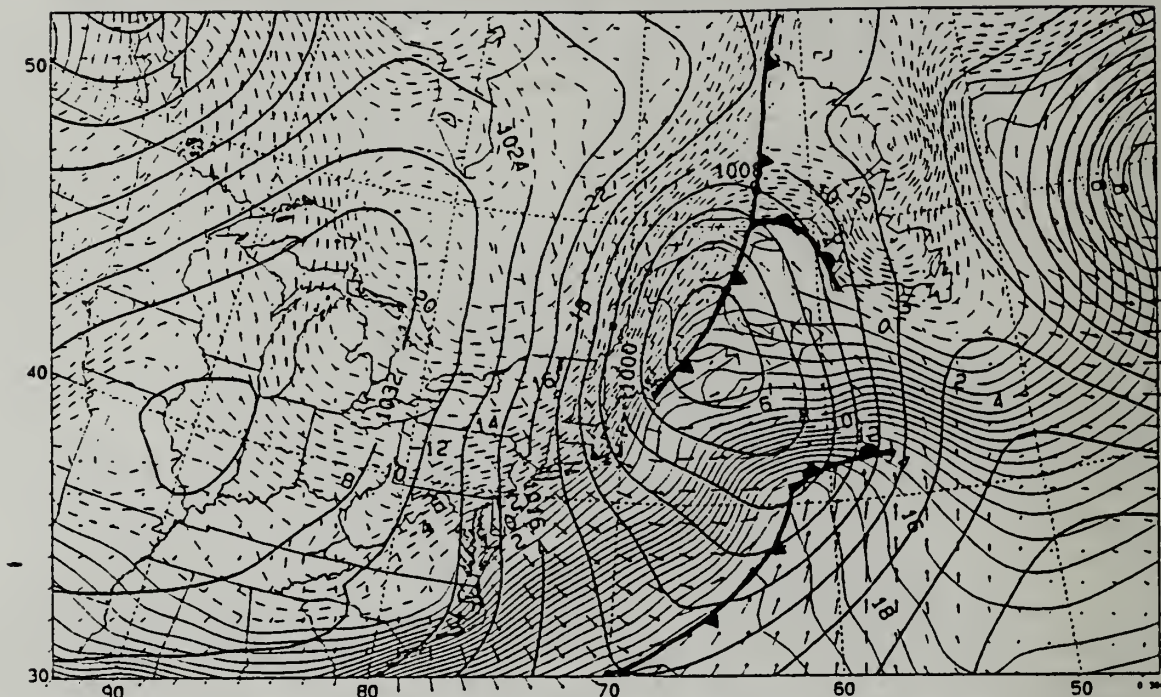


Figure 20. Sea level pressure and temperature as in Figure 5, except for 21/06Z January 1989.

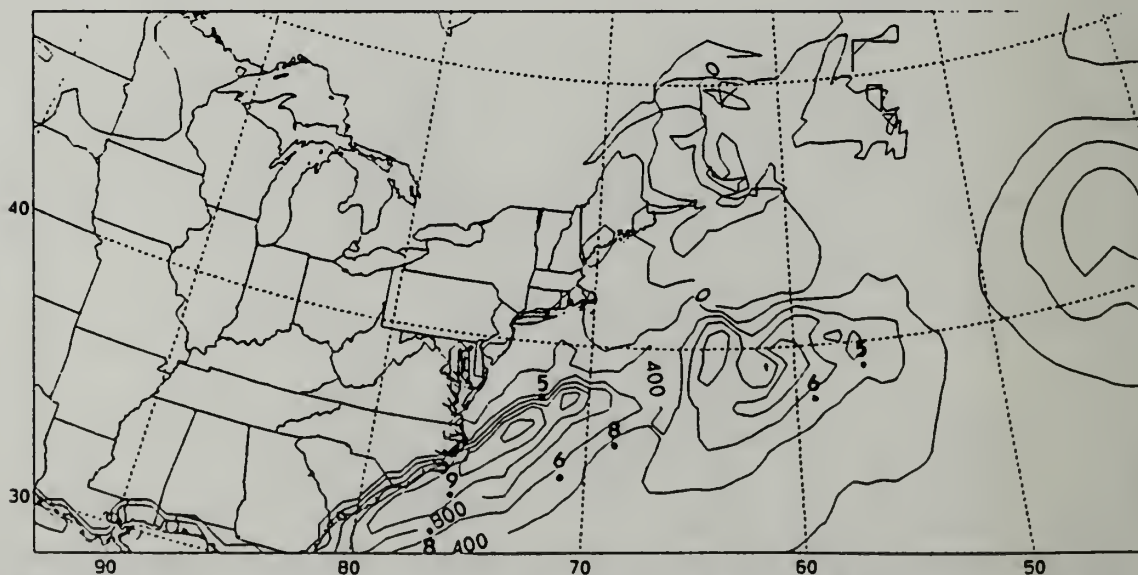


Figure 21. Surface latent heat flux as in Figure 9 except valid at 21/06Z January 1989.

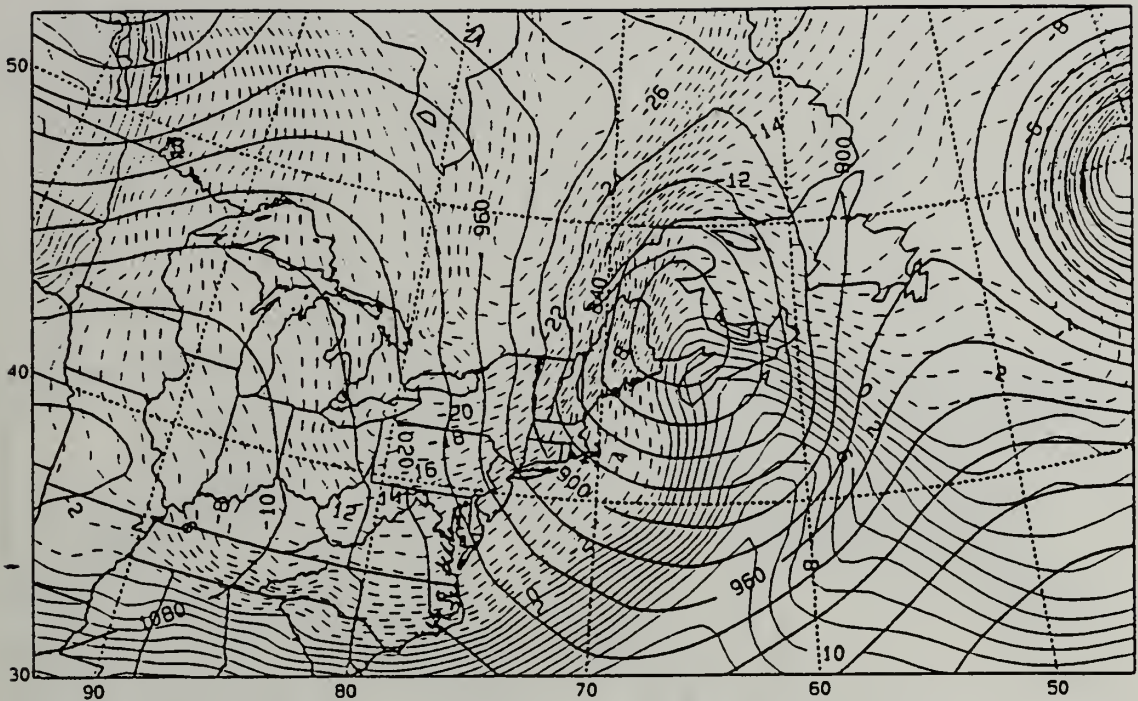


Figure 22. 900 mb geopotential height and temperature as in Figure 10, except 21/06Z January 1989.

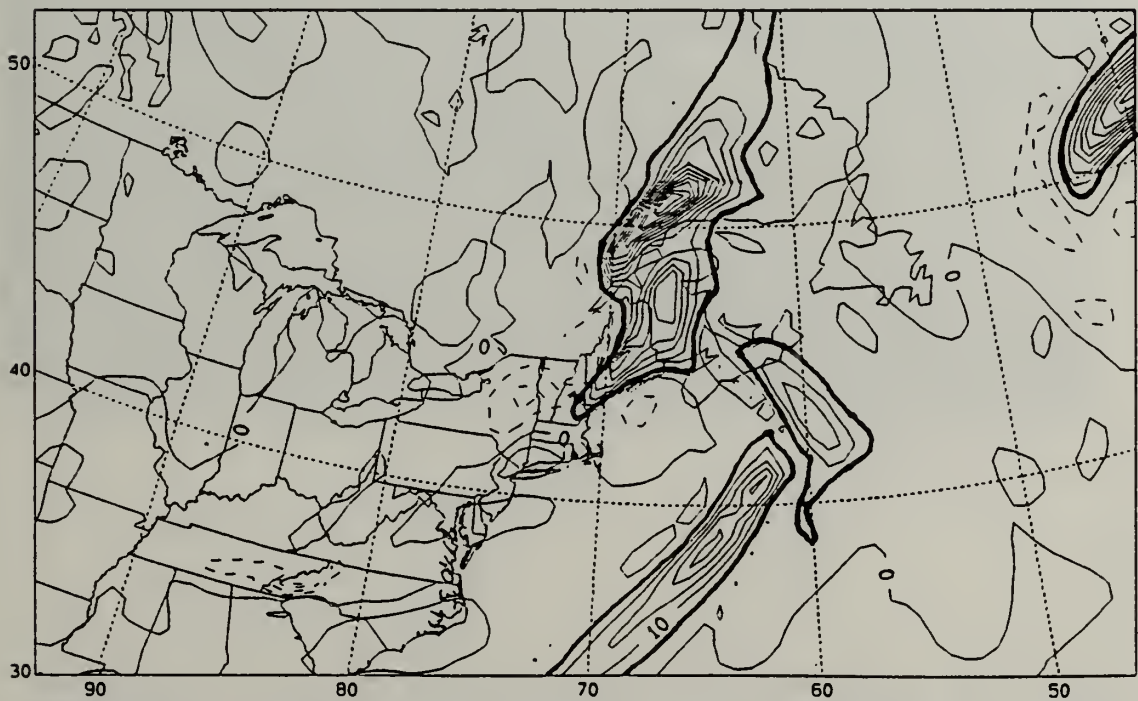


Figure 23. 900 mb frontogenesis, as in Figure 19, except 21/06Z January 1989.

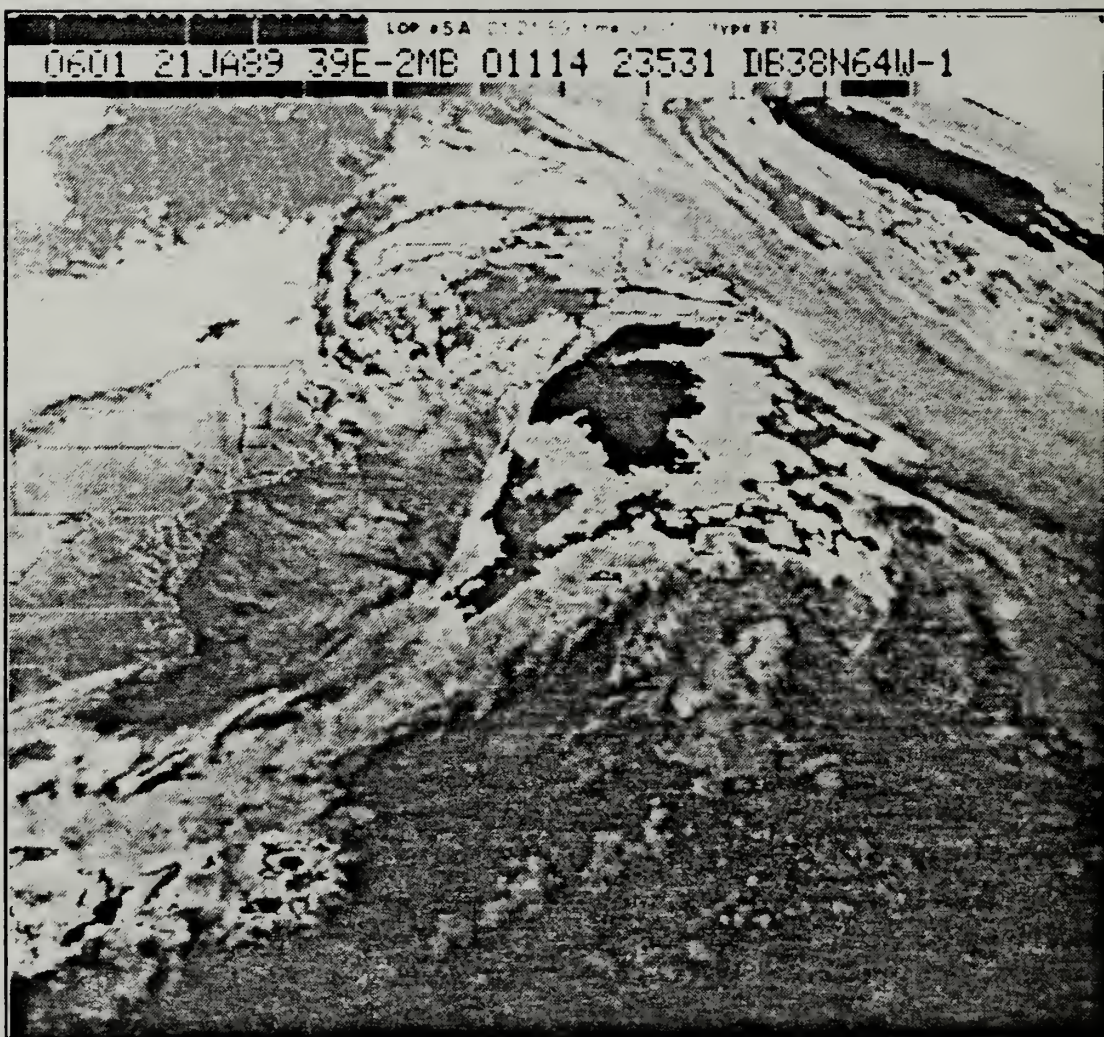


Figure 24. GOES enhanced IR satellite imagery at 21/0601Z.

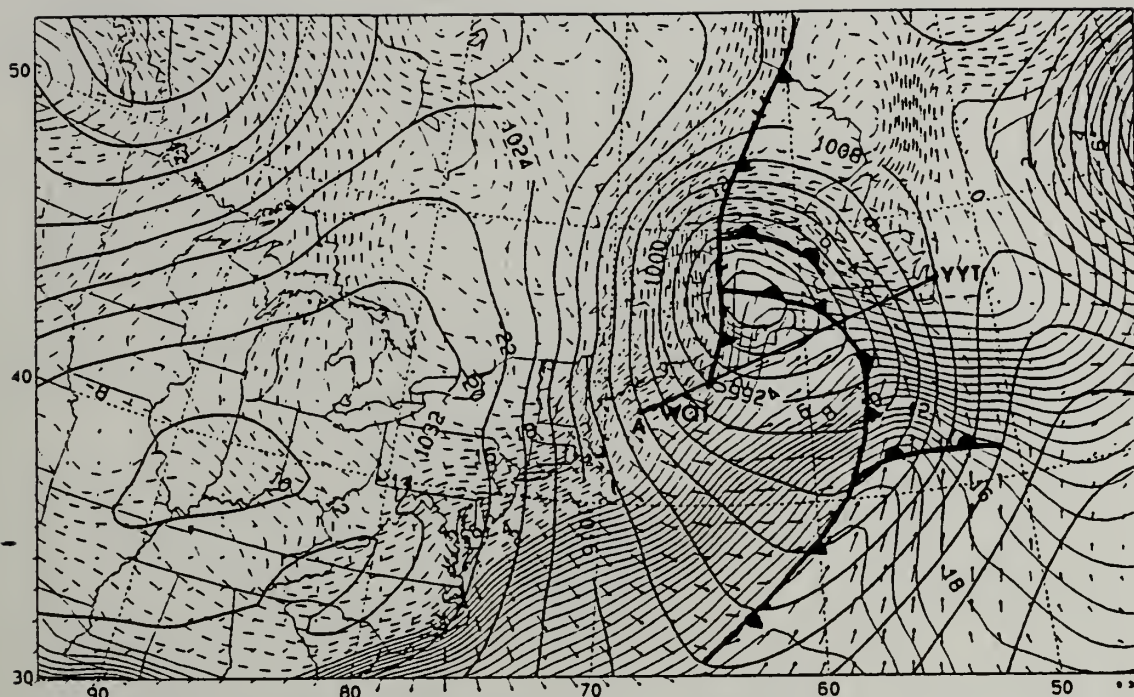


Figure 25. Sea level pressure and temperature as in Figure 5, except 21/12Z January 1989.

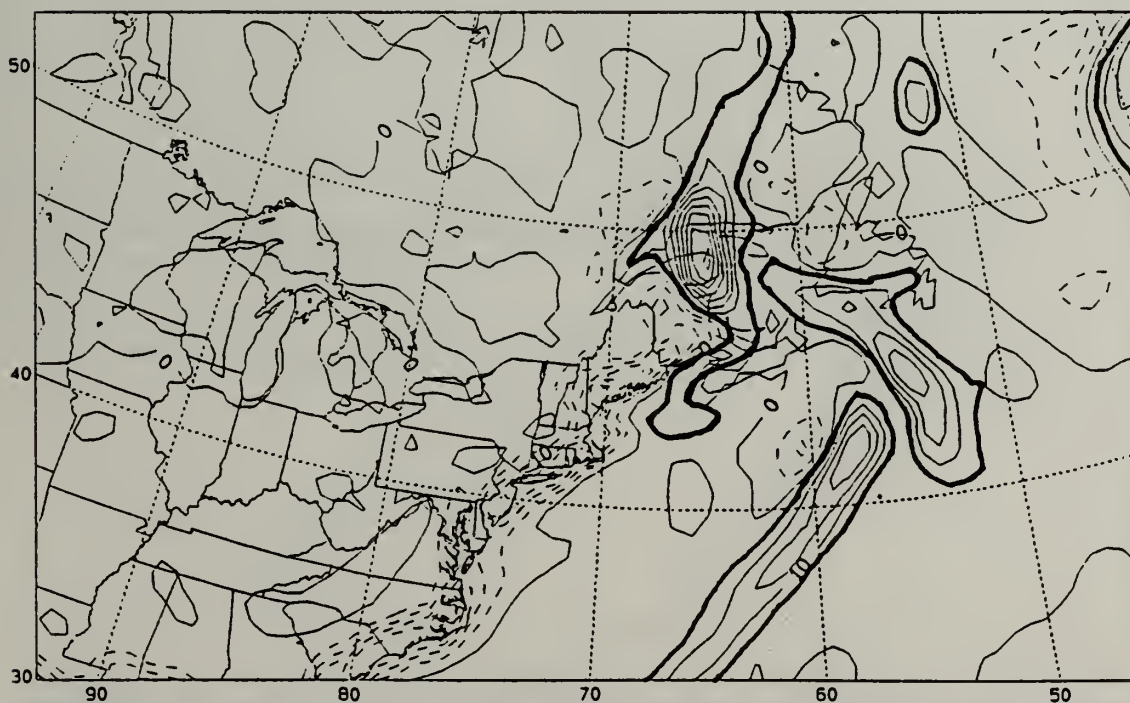


Figure 26. Surface frontogenesis as in Figure 8, except 21/12Z January 1989.

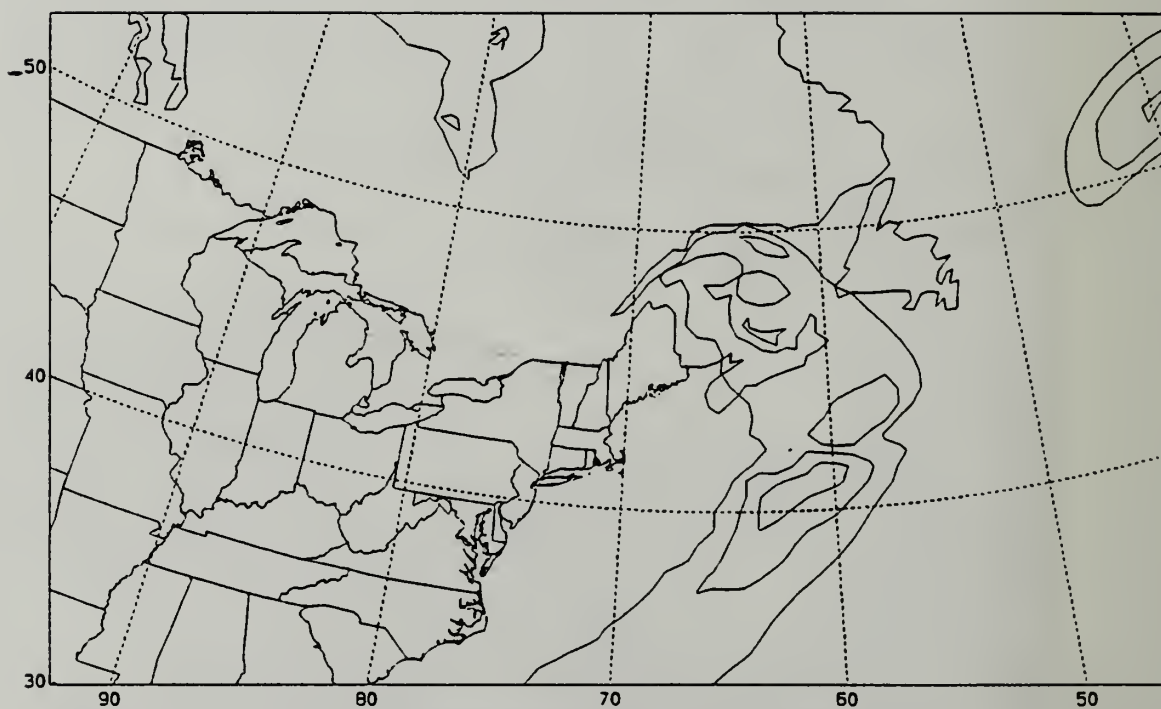


Figure 27. Total accumulated precipitation over the past 6 hours (contour interval 1 cm) valid 21/06Z January 1989.

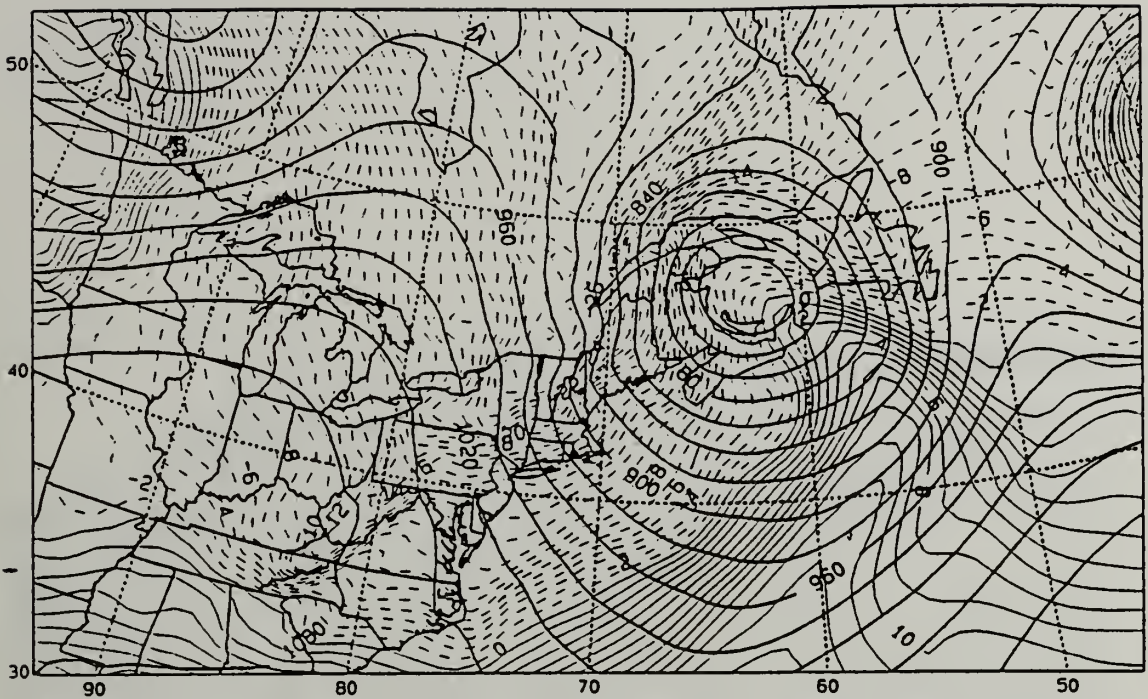


Figure 28. 900 mb geopotential height and temperature as in Figure 10, except 21/12Z January 1989.

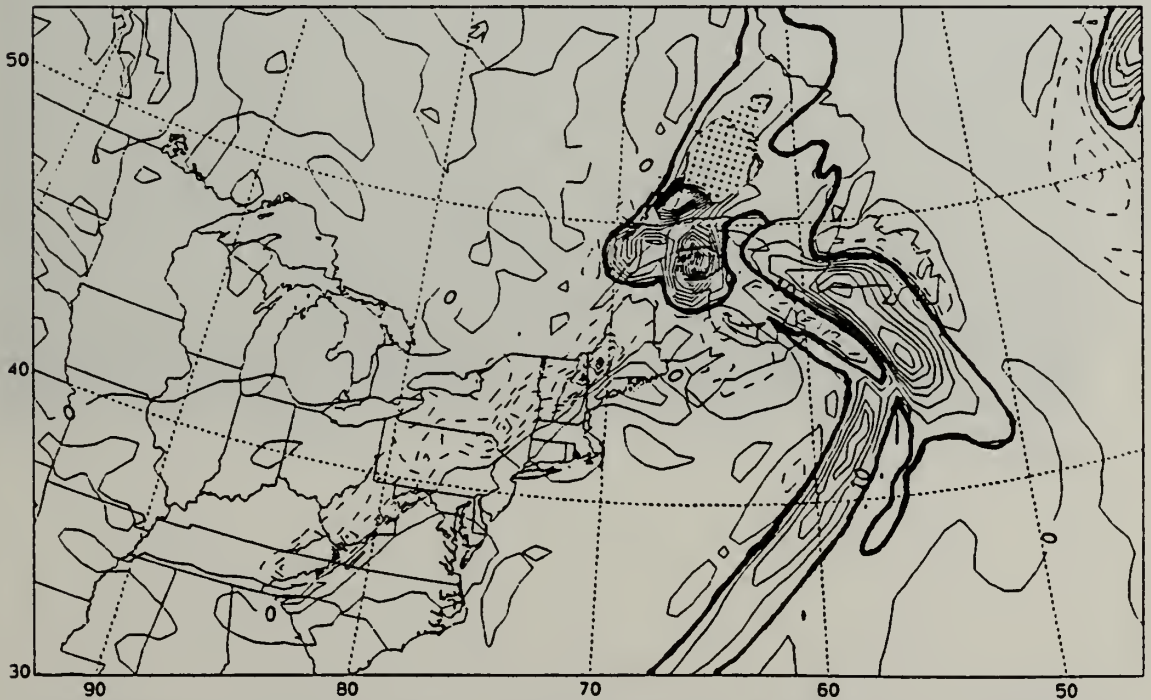


Figure 29. 900 mb frontogenesis as in Figure 19, except at 21/12Z January 1989. Stippling represents areas that are below ground level.

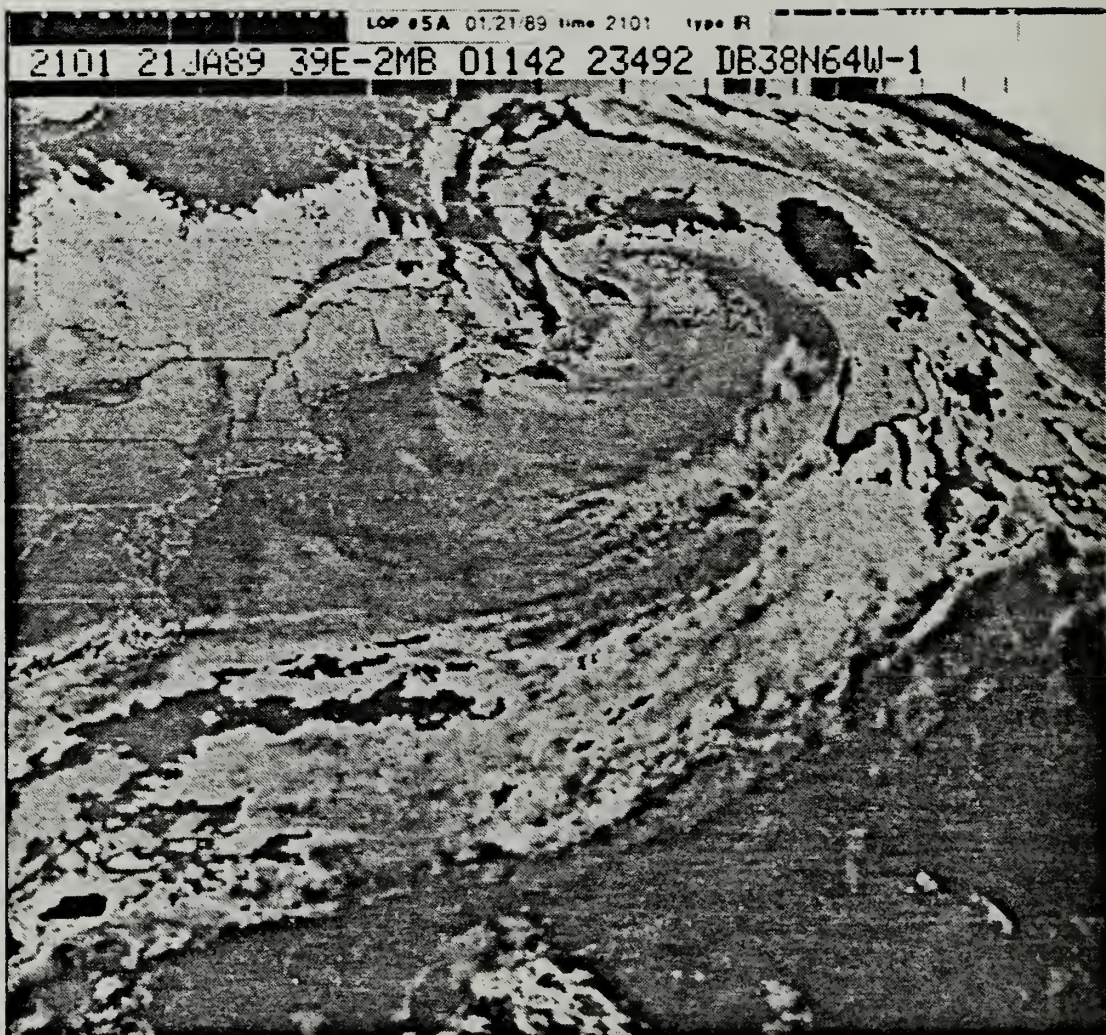


Figure 30. GOES enhanced IR satellite imagery at 21/1201Z January 1989.

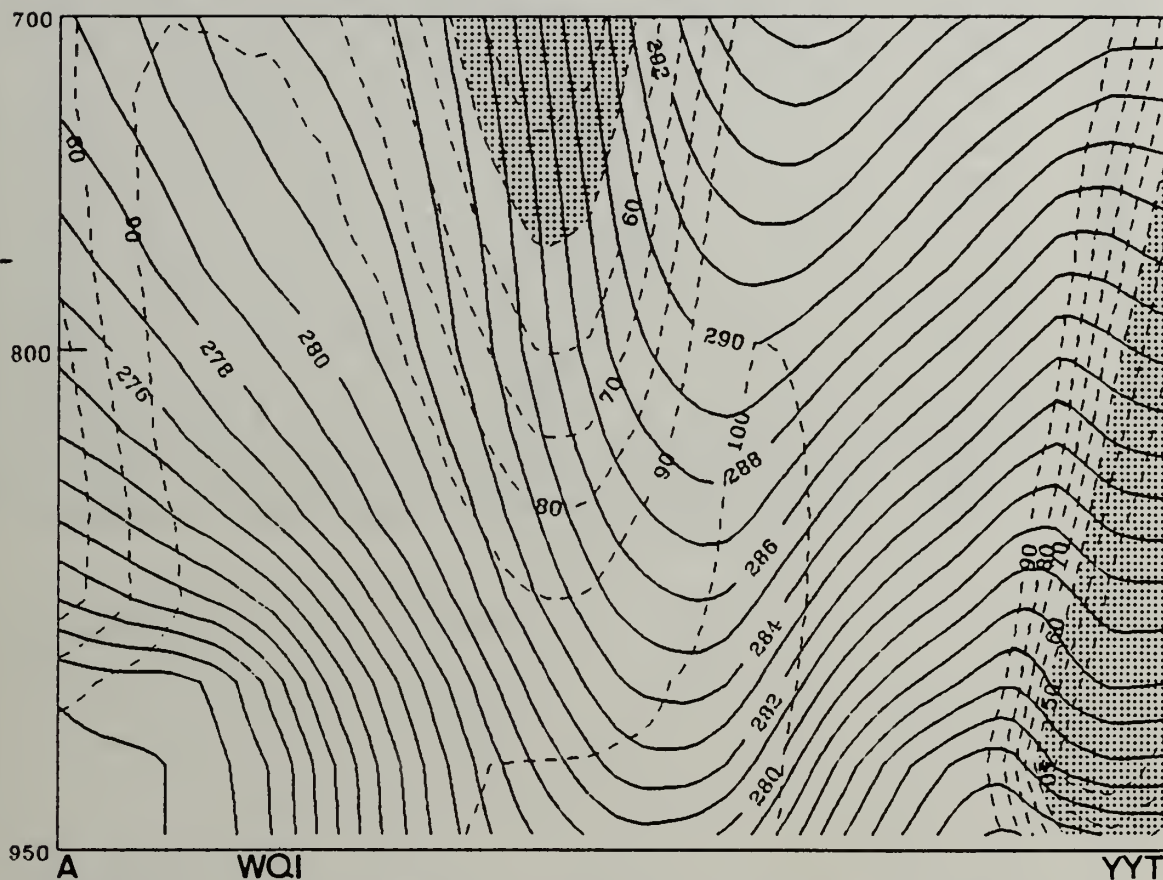


Figure 31. Model vertical cross section (dark solid, potential temperature; contour interval 1°C; light dashed, relative humidity; contour interval 10%; stippled greater than 50% RH) valid at 12/12Z January 1989.

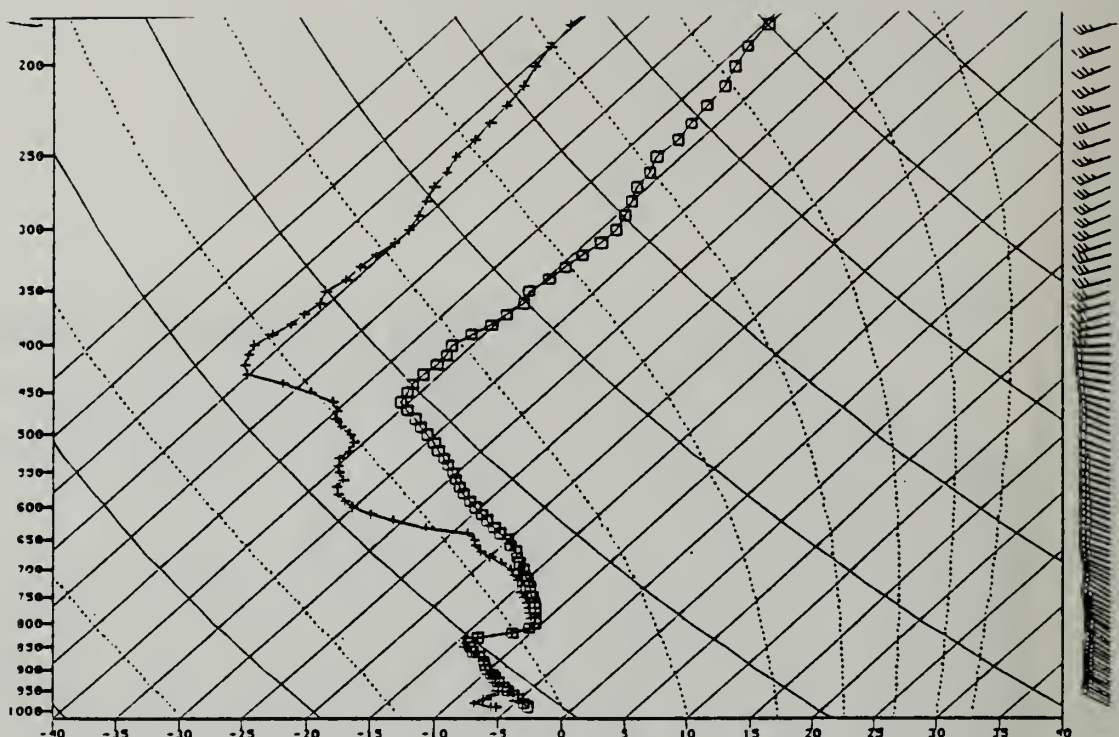


Figure 32. Observed sounding at Yarmouth, Nova Scotia (WQI) at 21/12Z January 1989 (boxes denote temperature, crosses denote dew point).

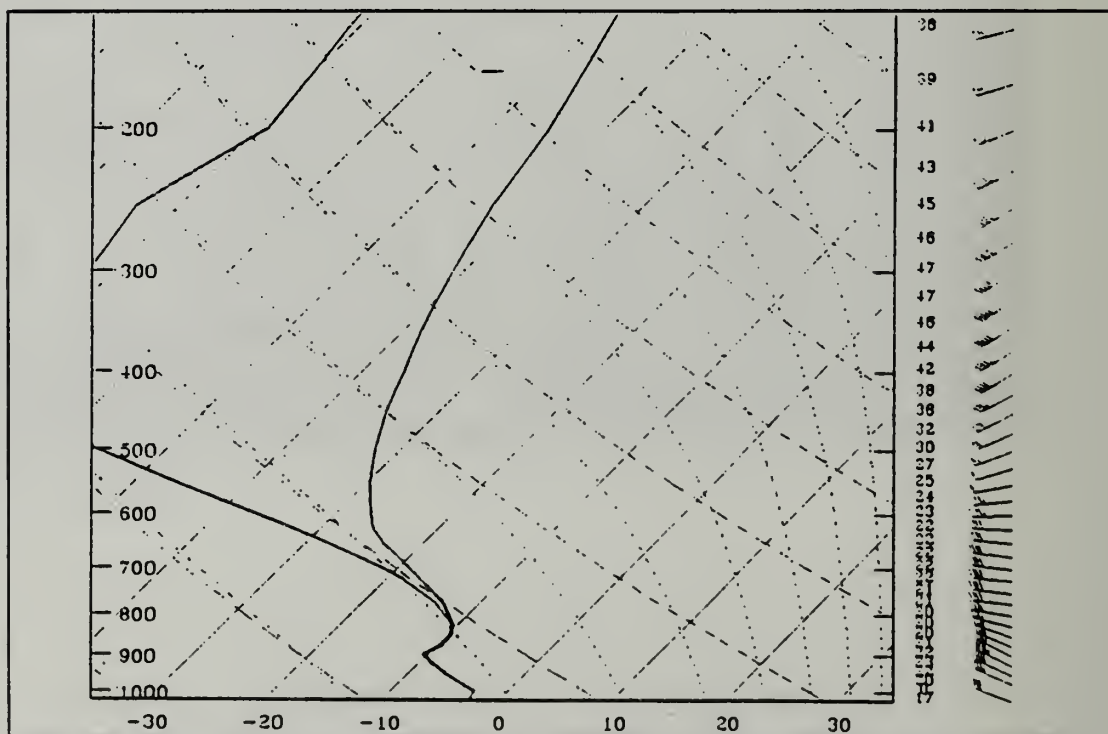


Figure 33. Model sounding for Yarmouth, Nova Scotia (WQI) at 21/12Z January 1989 (right line denotes temperature; left line denotes dew point).

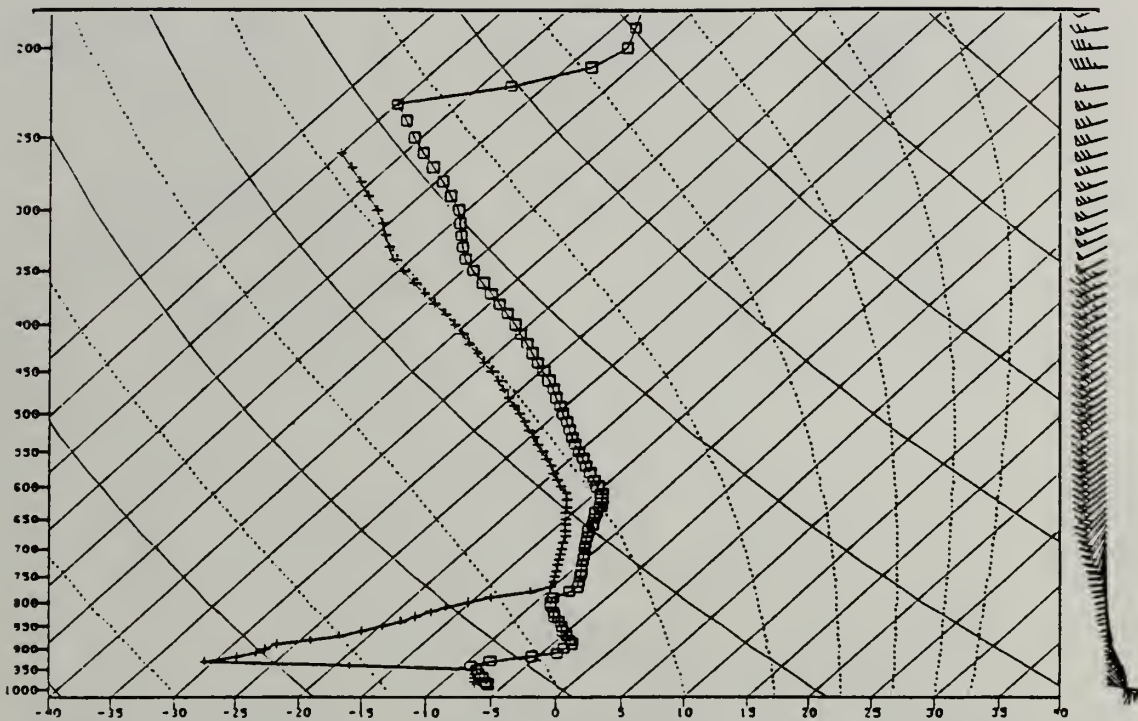


Figure 34. Observed sounding from St. Johns, Newfoundland (YYT) at 21/12Z January 1989 (boxes denote temperature; crosses denote dew point).

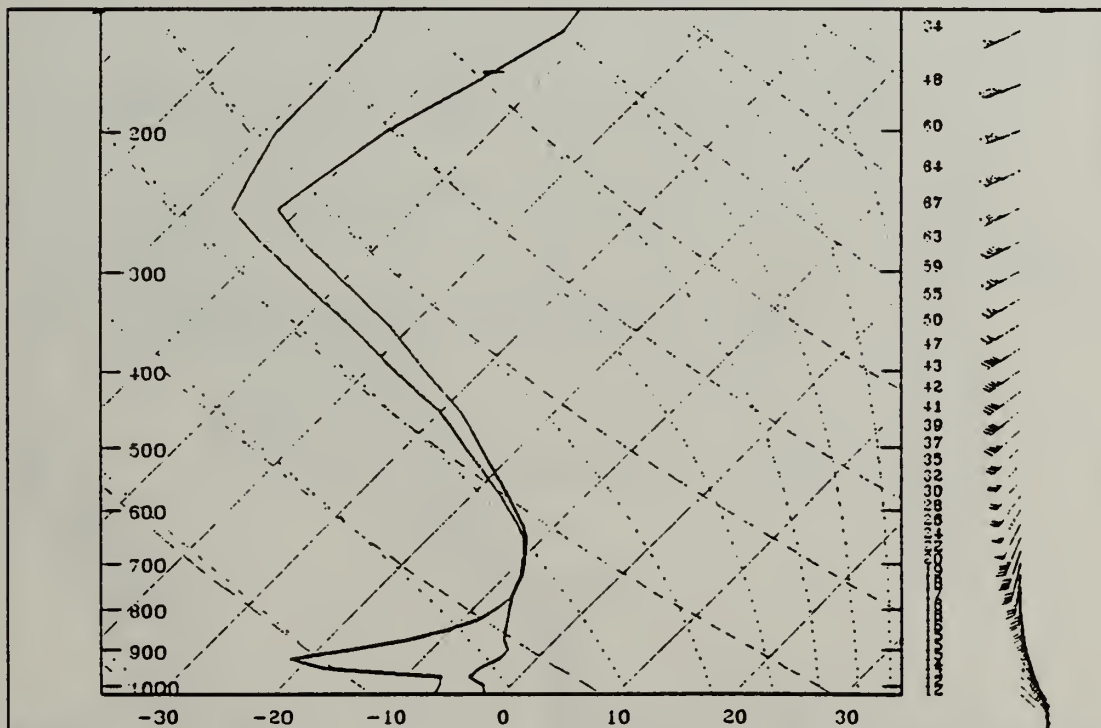


Figure 35. Model sounding for St. Johns, Newfoundland (YYT) at 21/12Z January 1989 (right line denotes temperature, left line denotes dew point).

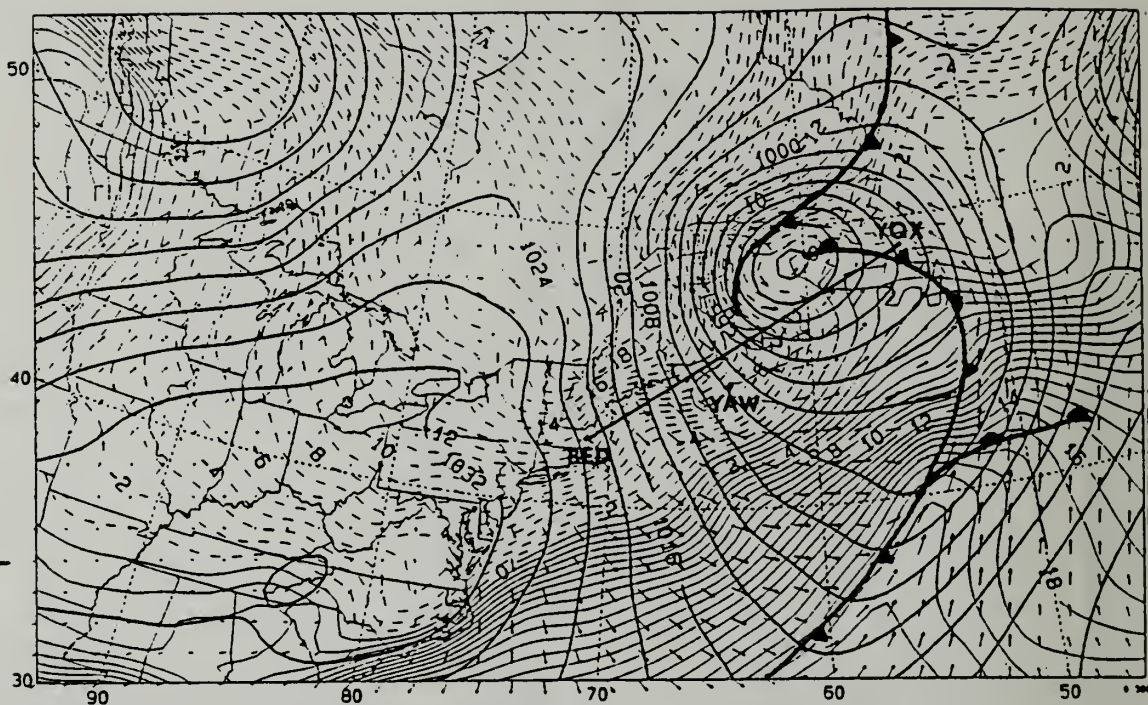


Figure 36. Sea level pressure and temperature as in Figure 5, except 21/18Z January 1989.

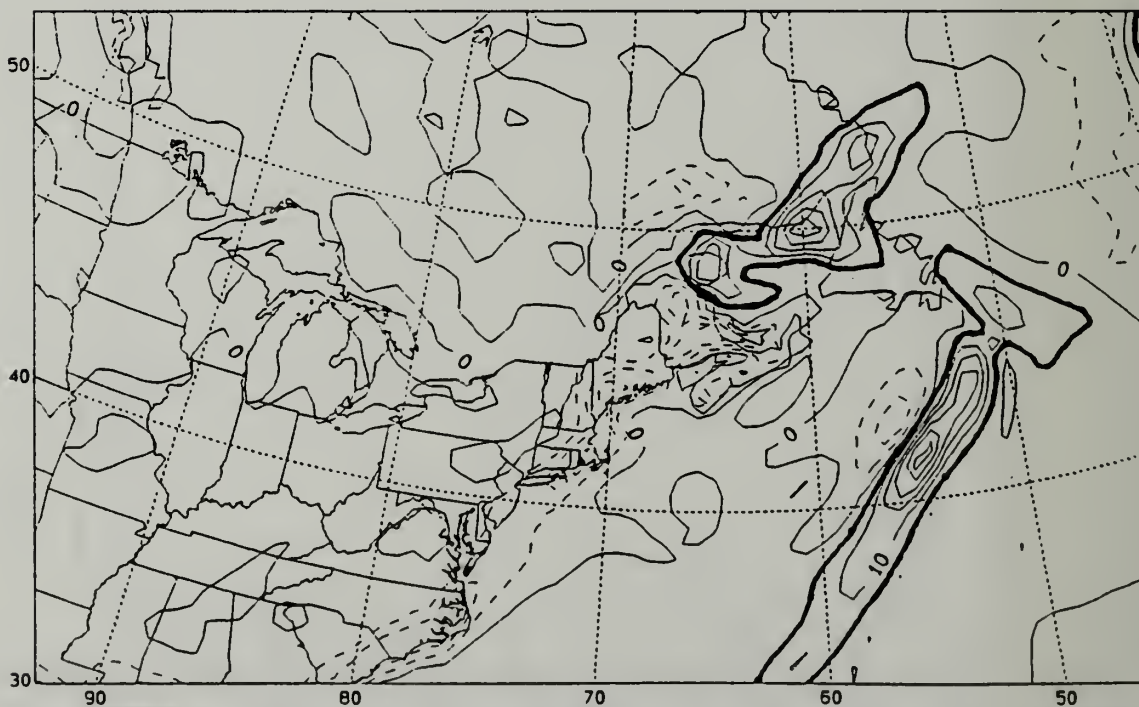


Figure 37. Surface frontogenesis as in Figure 8, except 21/18Z January 1989.

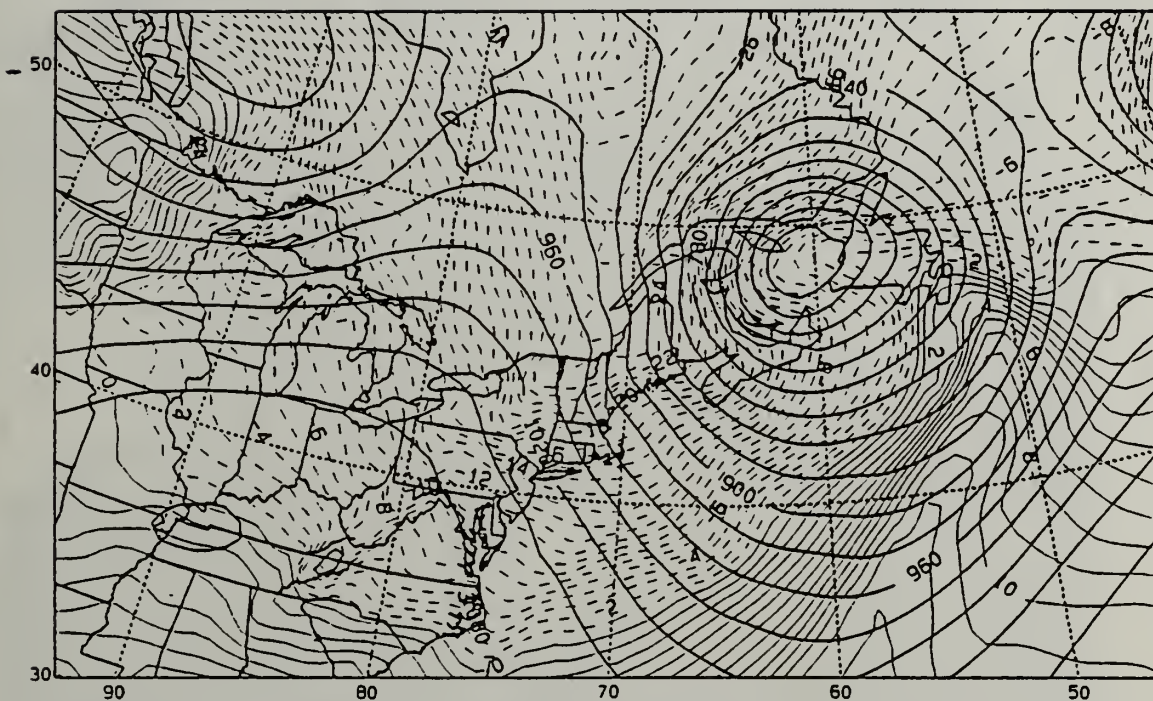


Figure 38. 900 mb geopotential height and temperature as in Figure 10, except 21/18Z January 1989.

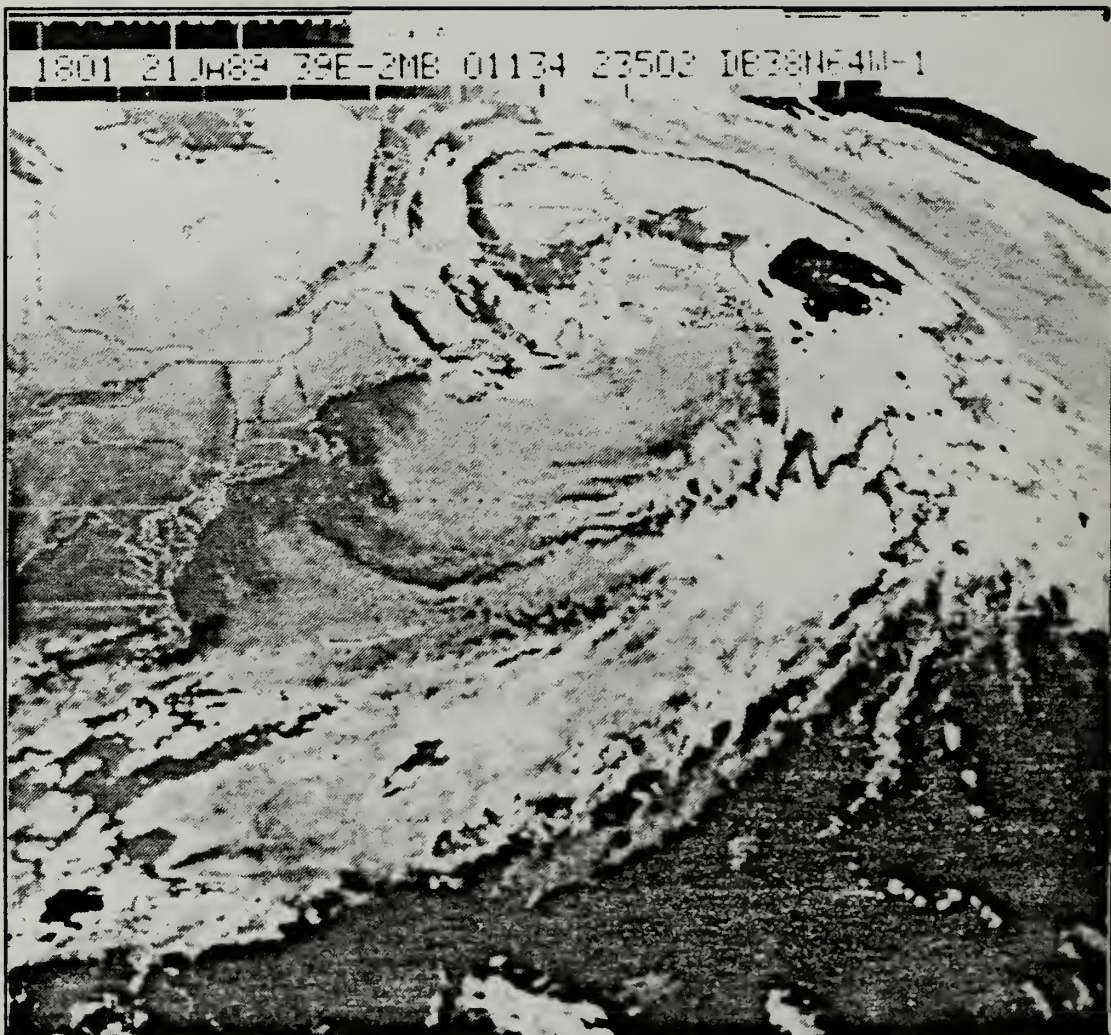


Figure 39. GOES enhanced IR satellite imagery at 21/1801Z January 1989.

1701 21JA89 393-42A 00902 17381 EC3

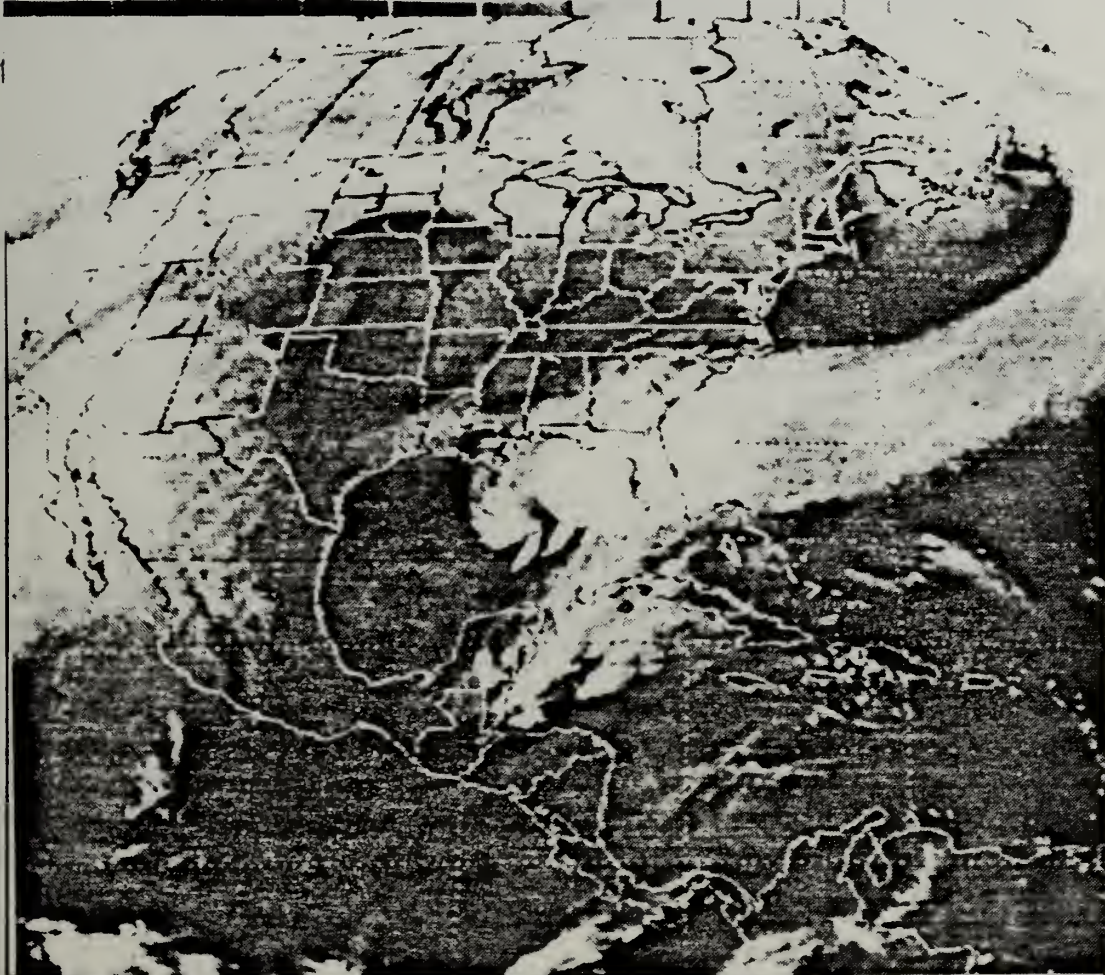


Figure 40. GOES water vapor imagery at 21/1701Z January 1989.

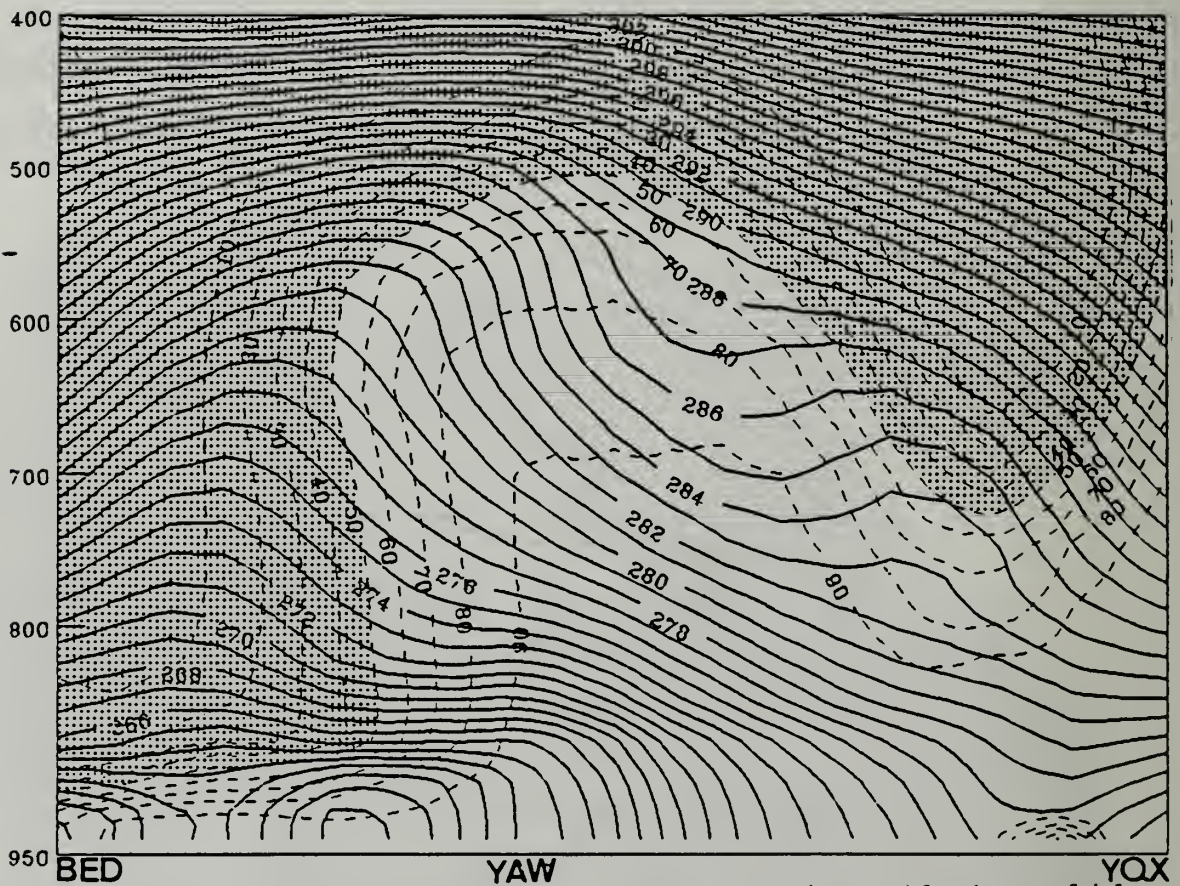


Figure 41. Model vertical cross section (dark solid, potential temperature; contour interval 1°C ; light dashed, relative humidity; contour interval 10%; stippled greater than 50% RH) valid at 21/18Z January 1989.

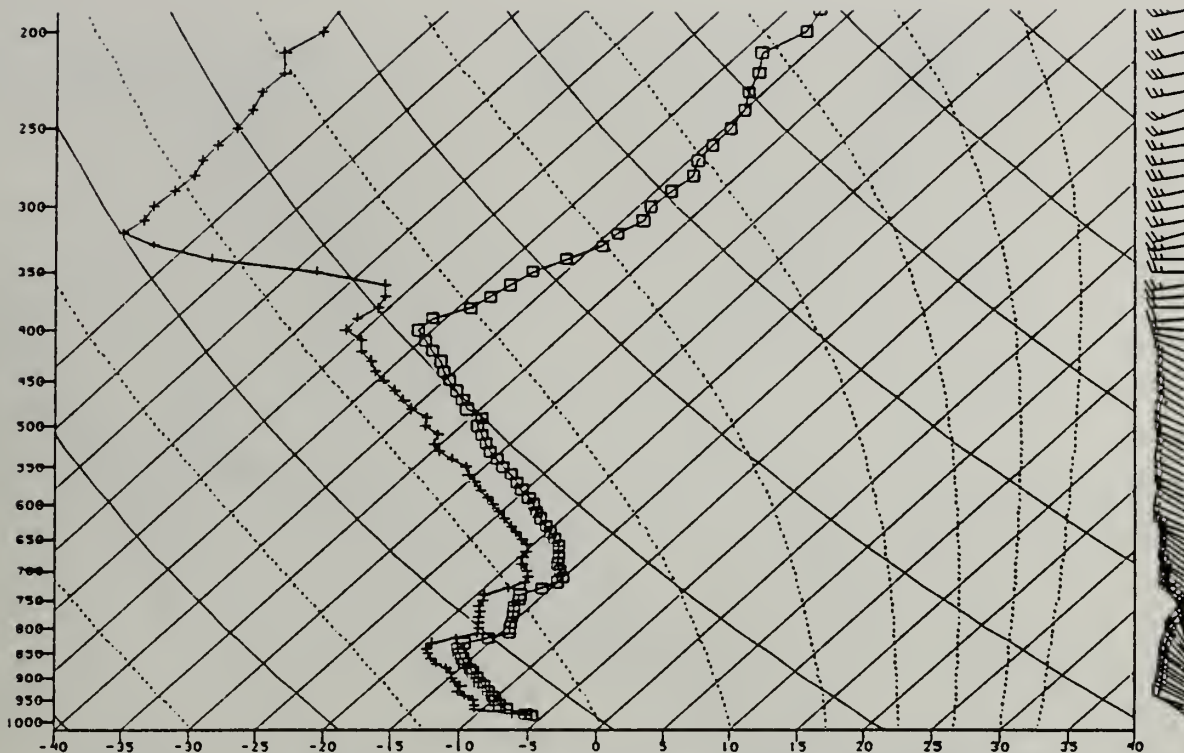


Figure 42. Observed sounding from Shearwater, Nova Scotia (YAW) at 21/18Z January 1989 (boxes denote temperature, crosses denote dew point).

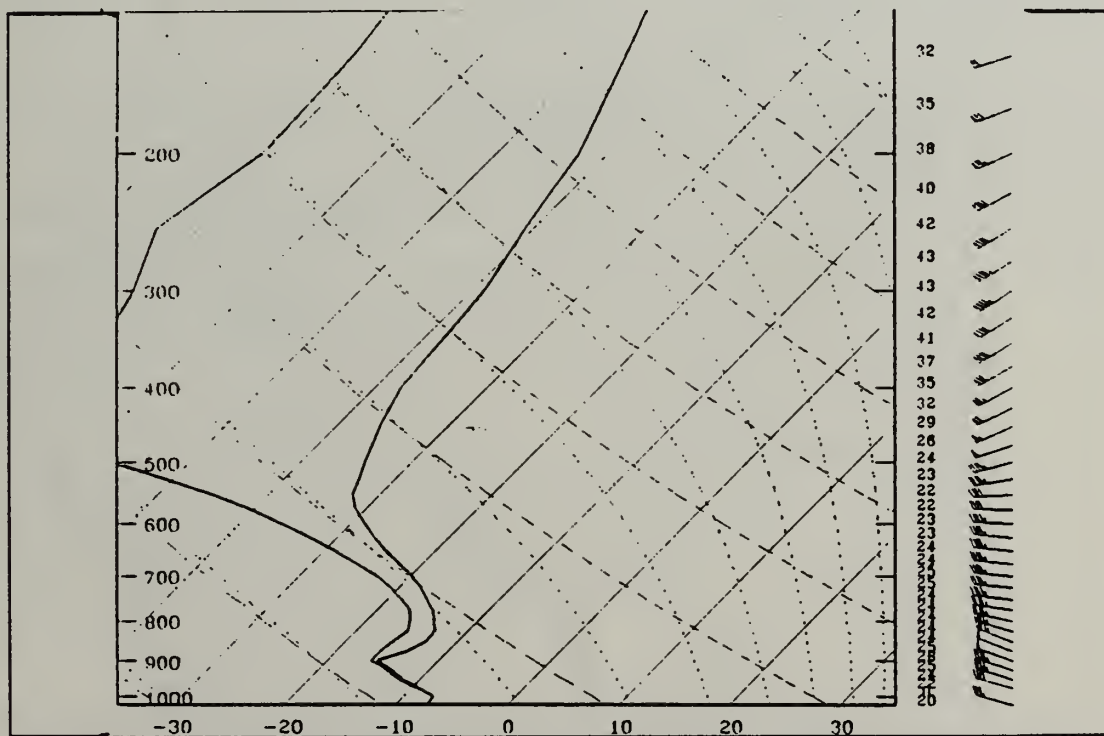


Figure 43. Model sounding for Shearwater, Nova Scotia (YAW) at 21/18Z January 1989 (right line denotes temperature, left line denotes dew point).

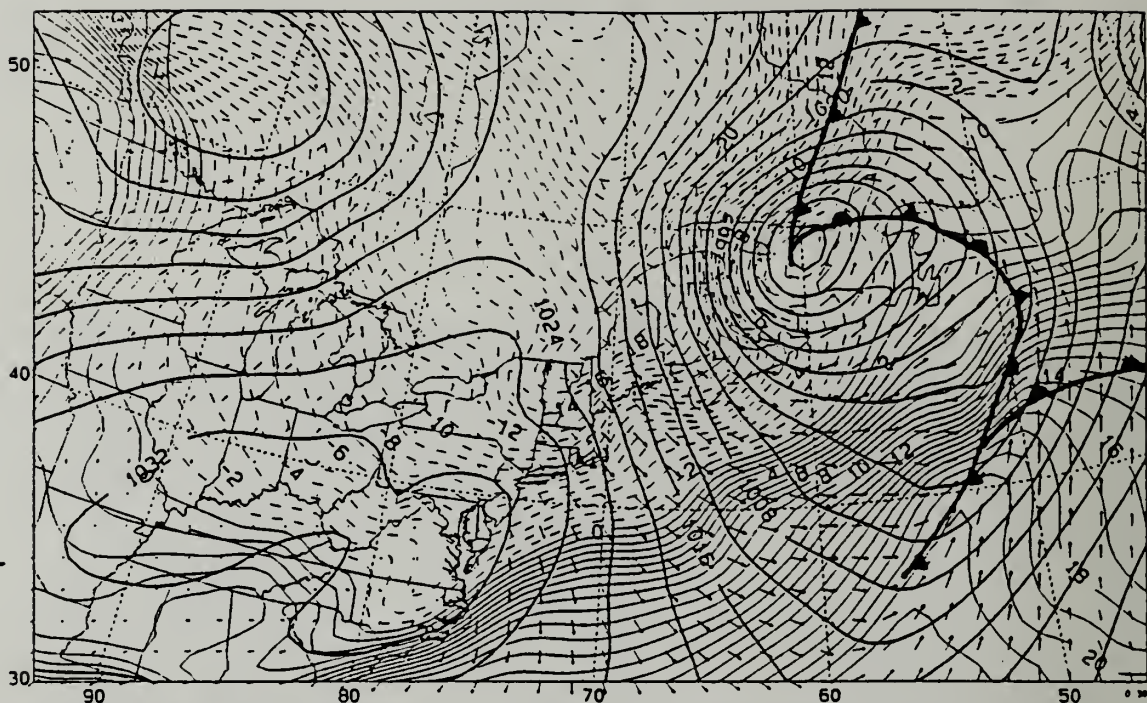


Figure 44. Sea level pressure and temperature as in Figure 5, except 21/21Z January 1989.

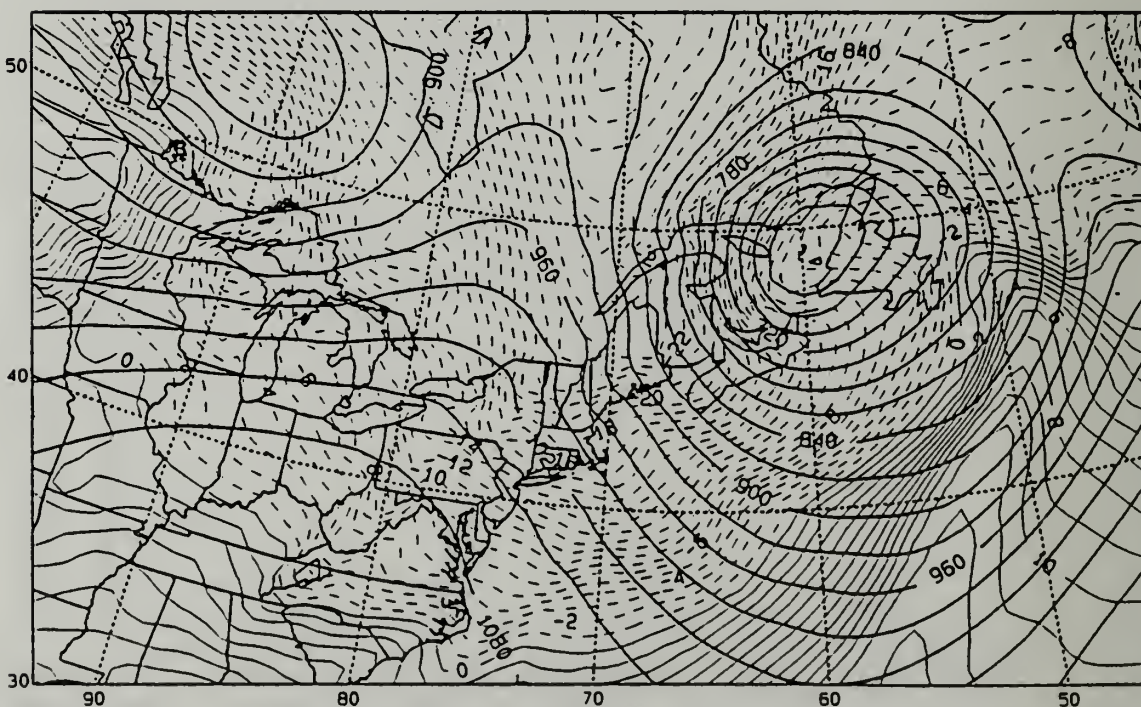
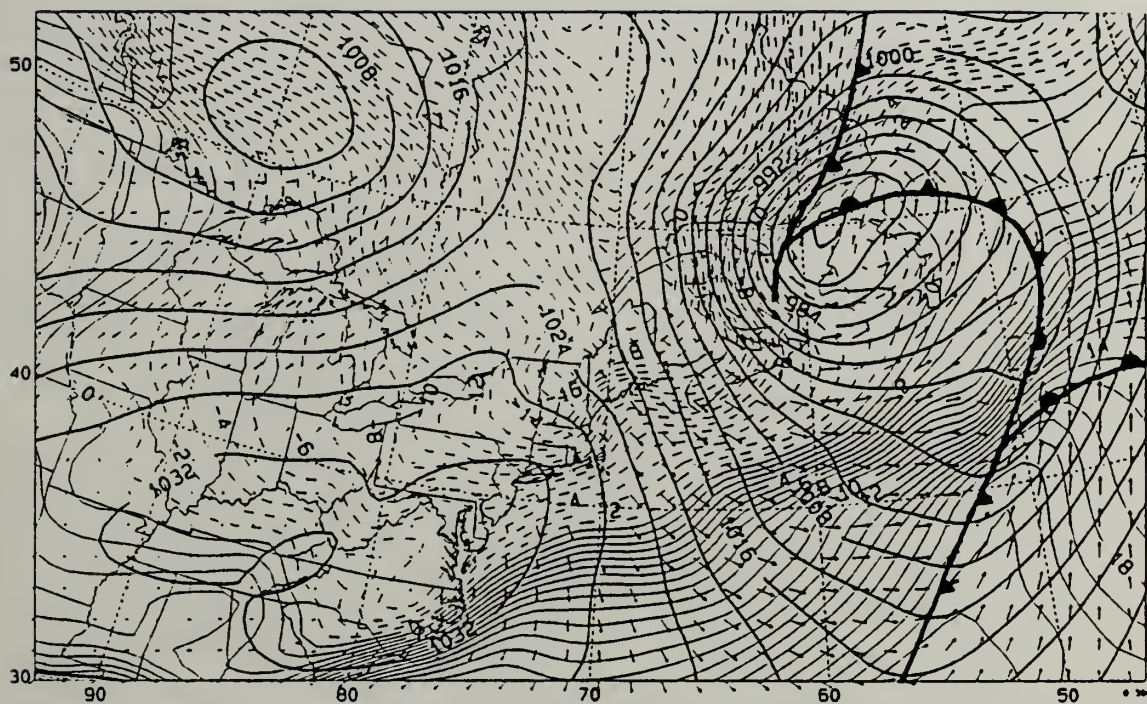


Figure 45. 900 mb geopotential height and temperature as in Figure 10, except 21/21Z January 1989.



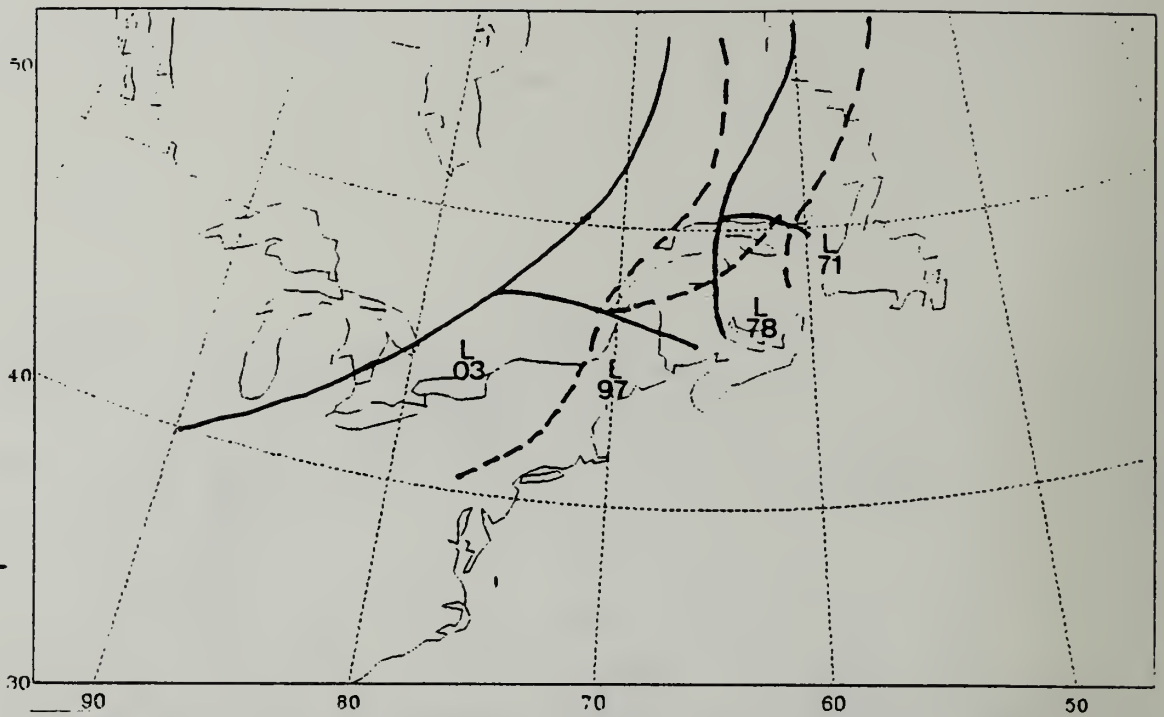


Figure 49. Composite Arctic front positions in twelve hour increments from 20/12Z to 22/00Z January 1989.

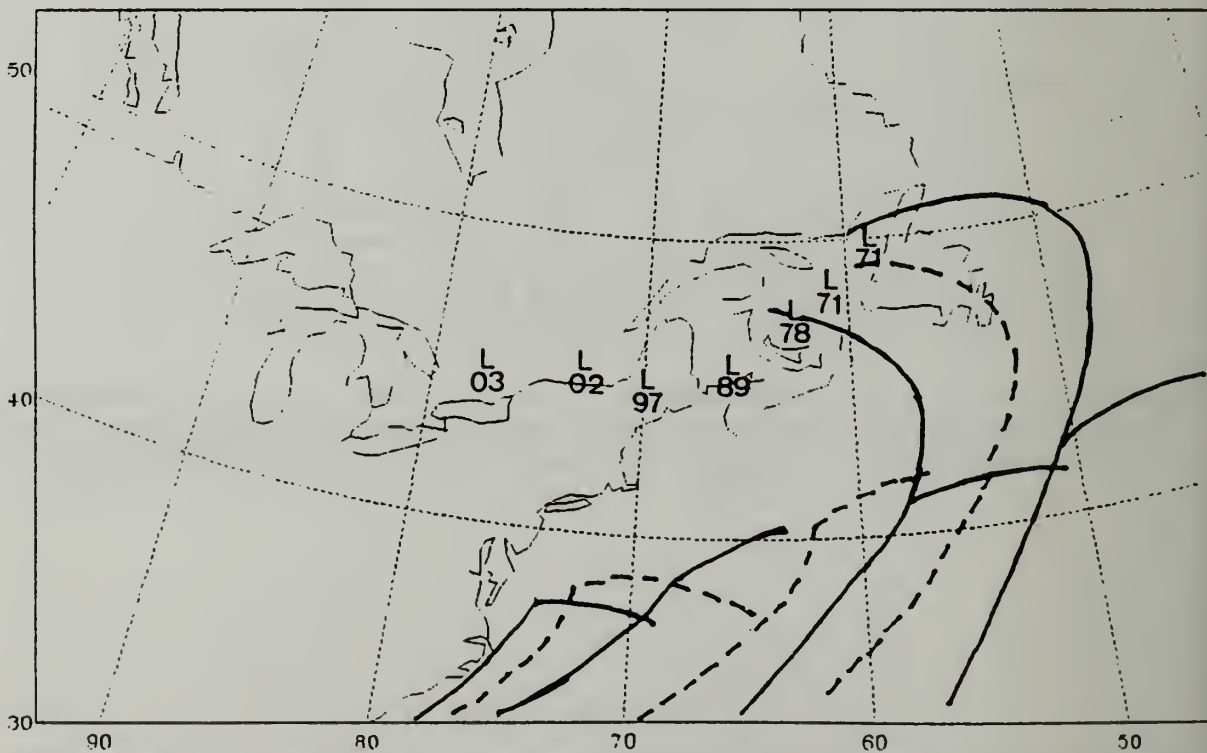


Figure 50. Composite coastal front positions in six hour increments from 20/12Z to 22/00Z January 1989.

LIST OF REFERENCES

- Bjerknes, J., and Solberg, H., 1922: Life Cycle of Cyclones and the Polar Front Theory of Atmospheric Circulation. *Geofys. Publ.*, **3**, No. 1, 1-18.
- Carlson, T.N., 1991: *Mid-Latitude Weather Systems*, Harper Collins Academic, New York, N.Y.
- Hadlock, R. and Kreitzberg, C.W., 1988: The Experiment on Rapidly Intensifying Cyclones Over the Atlantic (ERICA) field study: Objectives and Plans. *Bull. Amer. Meteo. Soc.*, **69**, 1309-1320.
- Hadlock, R., Hartnett E., and Forbes, G., 1989: The Experiment on Rapidly Intensifying Cyclones Over the Atlantic (ERICA) Field Phase Summary. [Available from ERICA Data Center, Department of Physics and Atmospheric Science, Drexel University, Philadelphia, Pennsylvania 19104.] 388 pp.
- Hirschberg, P.A., and Langland, R.H., 1992: The Effects of a Mesoscale Tropopause Undulation in a Numerical Simulation of the Cyclogenesis Event During ERICA IOP 5A. Fifth Conference on Mesoscale Processes January 5-10, 1992.
- Hodur, R.M., 1982: Description and Evaluation of NORAPS: The Navy Operational Regional Atmospheric Prediction System. *Mon. Wea. Rev.*, **110**, 1591-1602.
- Hodur, R.M., 1987: Evaluation of a Regional Model with an Update Cycle. *Mon. Wea. Rev.*, **115**, 2707-2718.
- Mass, C.F., and D.M. Shultz, 1993: The Structure and Evolution of a Simulated Midlatitude Cyclone Over Land. *Mon. Wea. Rev.*, **121**, 889-917.
- McGinnigle, J.B., 1988: The Development of Instant Occlusion in the North Atlantic. *Meteor. Mag.*, **117**, 325-340.
- Mullen, S.L., 1983: Explosive Cyclogenesis Associated with Cyclones in Polar Air Streams. *Mon. Wea. Rev.*, **111**, 1537-1553.
- Neiman. P.J., Shapiro, M.A., Donall, E.G., and Kreitzberg, C.W., 1990: The Diabatic Modification of an Extratropical Marine Cyclone Warm Sector by Cold Underlying Water. *Mon. Wea. Rev.*, **118**, 1576-1690.

- Neiman, P.J. and Shapiro, M.A., 1993: The Life Cycle of an Extratropical Marine Cyclone. Part I: Frontal-Cyclone Evolution and Thermodynamics Air-Sea Interactions. *Mon. Wea. Rev.*, **121**, 2153-2176.
- Sanders, F. and Gyakum, J.R., 1980: Synoptic-Dynamic Climatology of the "bomb". *Mon. Wea. Rev.*, **108**, 1589-1606.
- Shapiro, M.A., and Keyser, D., 1990: Fronts, Jet Stream and the Tropopause. *Extratropical Cyclones The Erik Palmen Memorial Volume*, American Meteorological Society.
- Spinelli, J.M., 1992: *An Investigation of the ERICA IOP 5A Cyclone*. M.S. thesis, Naval Postgraduate School, Monterey, California, December 1992.
- Uccellini, L.W., 1990: Processes Contributing to the Rapid Development of Extratropical Cyclones. *Extratropical Cyclones The Eric Palmen Memorial Volume*, C. Newton, and E.O. Holopainen, Eds., Amer. Meteor. Soc., 81-105.
- Wash, C.H., Peak, J.E., Calland, W.E., Cook, W.A., 1988: Diagnostic Study of Explosive Cyclogenesis During FFGE. *Mon. Wea. Rev.*, **116**, 431-451.
- Wash, C.H., Hale, R.A., Dobos, P.H., and Wright, E.J., 1992: Study of Explosive and Nonexplosive Cyclogenesis During FGGE. *Mon. Wea. Rev.*, **120**, 40-51.

INITIAL DISTRIBUTION LIST

| | No. copies |
|--|------------|
| 1. Defense Technical Information Center Cameron Station Alexandria VA 22304-6145 | 2 |
| 2. Library, Code 052 Naval Postgraduate School Monterey CA 93943-5002 | 2 |
| 3. Chairman (Code MR/Hy) Department of Meteorology Naval Postgraduate School Monterey CA 93943-5000 | 1 |
| 4. Professor C.H. Wash (Code MR/Wx) Department of Meteorology Naval Postgraduate School Monterey CA 93943-5000 | 3 |
| 5. Professor Paul A. Hirschberg (Code MR/Hs) Department of Meteorology Naval Postgraduate School Monterey CA 93943-5000 | 1 |
| 6. Commanding Officer Naval Eastern Oceanography Center Naval Air Station Norfolk VA 23511 Attn: LCDR Steven Cameron | 1 |
| 7. Director Naval Oceanography Division Naval Observatory 34th and Massachusetts Avenue NW Washington DC 20390 | 1 |
| 8. Commander Naval Oceanography Command Stennis Space Center MS 39529-5001 | 1 |
| 9. Commanding Officer Fleet Numerical Oceanography Center Monterey CA 93943-5001 | 1 |

10. Commanding Officer 1
Naval Oceanographic and Atmospheric
Research Laboratory
Stennis Space Center
MS 39529-5004
11. Chief of Naval Research 1
800 N. Quincy Street
Arlington VA 22217

DUDLEY KNOX LIBRARY
NAVAL POSTGRADUATE SCHOOL
MONTEREY CA 93940-5101



DUDLEY KNOX LIBRARY



3 2768 00311307 7